AD-A083 231 AEROSPACE CORP EL SEGUNDO CA ENGINEERING GROUP F/G 20/3
AN ANALYTICAL INTEGRATION OF THE AVERAGED EQUATIONS OF VARIATIO--ETC(U)
OCT 79 C C CHAO FU4701-79-C-0080
UNCLASSIFIED TR-0080(5473-03)-1 SD-TR-80-12 NL

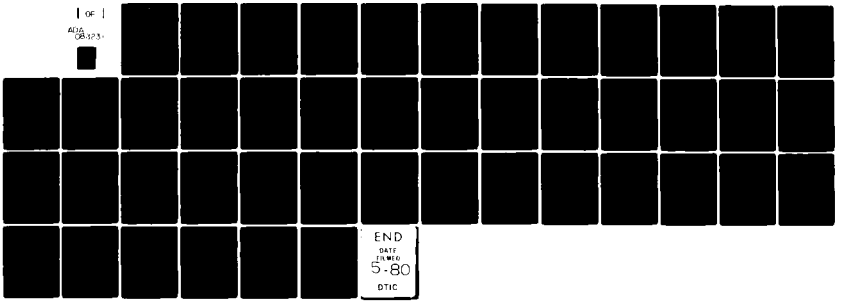

END
DATE FILMED
5-80
DTIC

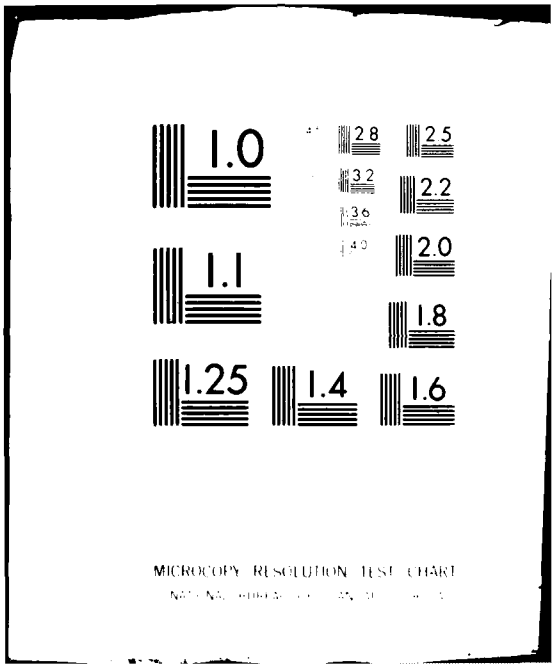
1.0
2.8
2.5
3.2
2.2
3.6
4.0
2.0
1.1
1.8
1.25
1.4
1.6
MICROCOPY RESOLUTION TEST CHART

REPORT SD-TR-80-12

LEVEL II

12



# An Analytical Integration of the Averaged Equations of Variation Due to Sun-Moon Perturbations and its Application

Prepared by C. C. CHAO
Orbital and Environmental Analysis Office
Engineering Group
The Aerospace Corporation
El Segundo, Calif. 90245

*October 1979*

Final Report
(Oct. 1978-March 1979)



Prepared for

SPACE DIVISION
AIR FORCE SYSTEMS COMMAND
Los Angeles Air Force Station
P.O. Box 92960, Worldway Postal Center
Los Angeles, Calif. 90009

This final report was submitted by The Aerospace Corporation, El Segundo, Ca. 90245, under Contract F04701-79-C-0080 with the Space and Missile Systems Organization, Deputy for Space Navigation Systems, P.O. Box 92960, Worldway Postal Center, Los Angeles, Ca. 90009. It was reviewed and approved for The Aerospace Corporation by A.J. Boardman, Engineering Group, and P.L. Swanson, Programs Group. Col. D.W. Henderson, SAMSO/YE, was the project engineer.

This report has been reviewed by the Public Affairs Office (PAS) and is releasable to the National Technical Information Service (NTIS). At NTIS, it will be available to the general public, including foreign nationals.

This technical report has been reviewed and is approved for publication. Publication of this report does not constitute Air Force approval of the report's findings or conclusions. It is published only for the exchange and stimulation of ideas.

Brian L Masson

BRIAN L. MASSON, Capt, USAF
Chief, Operations Division
Directorate of Satellite Control System

RALEIGH E. DEW, Lt Col, USAF
Director, Satellite Control System
Navstar Global Positioning System

FOR THE COMMANDER

Donald W. Henderson

DONALD W. HENDERSON, Colonel, USAF
Deputy for Space Navigation Systems
Navstar Global Positioning System

UNCLASSIFIED

SECURITY CLASSIFICATION OF THIS PAGE (When Data Entered)

| (18) (19) REPORT DOCUMENTATION PAGE | | READ INSTRUCTIONS BEFORE COMPLETING FORM |
|---|---|---|
| 1. REPORT NUMBER<br>SD-TR-80-12 | 2. GOVT ACCESSION NO. | 3. RECIPIENT'S CATALOG NUMBER |
| 4. TITLE (and Subtitle)<br>(6) AN ANALYTICAL INTEGRATION OF THE AVERAGED EQUATIONS OF VARIATION DUE TO SUN-MOON PERTURBATIONS AND ITS APPLICATION | | 5. TYPE OF REPORT & PERIOD COVERED<br>(9) Final Report<br>Oct 1978-Mar 1979 |
| | | 6. PERFORMING ORG. REPORT NUMBER<br>(14) TR-0080(5473-03)-1 |
| 7. AUTHOR(s)<br>(10) C. C. Chao | | 8. CONTRACT OR GRANT NUMBER(s)<br>(15) F04701-79-C-0080 |
| 9. PERFORMING ORGANIZATION NAME AND ADDRESS<br>The Aerospace Corporation<br>El Segundo, California 90245 | | 10. PROGRAM ELEMENT, PROJECT, TASK AREA & WORK UNIT NUMBERS |
| 11. CONTROLLING OFFICE NAME AND ADDRESS<br>(11) Space and Missile Systems Organization<br>Air Force Systems Command<br>Los Angeles, California 90009 | | 12. REPORT DATE<br>October 1979<br>13. NUMBER OF PAGES<br>43 |
| 14. MONITORING AGENCY NAME & ADDRESS (if different from Controlling Office)<br>(12) 46 | | 15. SECURITY CLASS. (of this report)<br>Unclassified<br>15a. DECLASSIFICATION/DOWNGRADING SCHEDULE |

16. DISTRIBUTION STATEMENT (of this Report)

Approved for public release; distribution unlimited.

17. DISTRIBUTION STATEMENT (of the abstract entered in Block 20, if different from Report)

18. SUPPLEMENTARY NOTES

19. KEY WORDS (Continue on reverse side if necessary and identify by block number)

General perturbation method
Orbit maintenance algorithm

20. ABSTRACT (Continue on reverse side if necessary and identify by block number)

The perturbed variations of the motion of earth satellites due to the sun and the moon are derived from a singly averaged disturbing function. A first-order solution is obtained by analytically integrating the equations of variation including $J_2^2$, $J_2^2$, $J_3^2$, and $J_4^2$. The literal expansions are carried out by computer in terms of classical elements. The secular part of the first-order solution is included in the reference orbit. The orbits of the sun and the moon

DD FORM 1473 (FACSIMILE)

411 279

UNCLASSIFIED

SECURITY CLASSIFICATION OF THIS PAGE (When Data Entered)

19. KEY WORDS (Continued)

20. ABSTRACT (Continued)

are assumed circular, and the motion of the moon is converted to the earth equatorial system with certain approximations.

Results based on the GPS (Global Positioning System) satellites compare favorably with numerical integration for time spans of up to three years. An algorithm applying the first-order solution has been developed to achieve the desired strategy of orbit maintenance for the GPS Phase III system. The analytical solutions provide insight into the long-term (10-yr) variations of the orbit elements of GPS satellites.

CONTENTS

## FIGURES

## TABLES

# AN ANALYTICAL INTEGRATION OF THE AVERAGED EQUATIONS OF VARIATION DUE TO SUN-MOON PERTURBATIONS AND ITS APPLICATION

C.C. Chao

The perturbed variations of the motion of earth satellites due to the sun and the moon are derived from a singly averaged disturbing function. A first-order solution is obtained by analytically integrating the equations of variation including $J_2$, $J_2^2$, $J_3$, and $J_4$. The literal expansions are carried out by computer in terms of classical elements. The secular part of the first-order solution is included in the reference orbit. The orbits of the sun and the moon are assumed circular, and the motion of the moon is converted to the earth equatorial system with certain approximations.

Results based on the GPS (Global Positioning System) satellites compare favorably with numerical integration for time spans of up to three years. An algorithm applying the first-order solution has been developed to achieve the desired strategy of orbit maintenance for the GPS Phase III system. The analytical solutions provide insight into the long-term (10-yr) variations of the orbit elements of GPS satellites.

## INTRODUCTION

The need to rapidly predict the long-period and secular perturbations of artificial satellite orbits increases as more high-altitude satellites with long life spans, such as the GPS (Global Positioning System) satellites, are launched into orbit. By the late 1980s, a total of 18 GPS satellites will be orbiting around the earth for 12-hr periods. The ground tracks covered by these satellites are required to repeat every 24 hr to insure a continuous global coverage. Regular orbit maneuvers must be performed to maintain the specified repeating coverage against long-term perturbations due to the sun-moon attractions and the earth gravitational

potential. The desired strategy for orbit maintenance maneuvers, as requested by the GPS program office, is to minimize the total number of such maneuvers during the life span of these satellites. To achieve this strategy, an analytical solution which predicts the long-term variations of the orbit parameters is highly desirable in determining the proper $\Delta V$ at the time of each maneuver.

During the past two decades, efforts have been made by many researchers to develop general perturbation theories for the long-term variations of planetary and earth orbiters. To name a few, Kozai[1], Kaula[2], Musen[3], Murphy[4], and Estes[5] have either developed or applied analytical solutions to the problem of third-body perturbation for artificial satellites. Kaufman[6], Uphoff[7], and Cefola, et al.[8], have applied the method of averaging, in a numerical approach, to the prediction of the long-term variations of planetary and lunar orbiters. Their results show a tremendous improvement in speed over that obtained from the n-body numerical integration, yet they do not give the analytical expressions which are preferred in this application.

The purpose of this analysis is to further expand the singly averaged disturbing function of third-body perturbation arrived at by Kaufman in terms of classical elements, and to apply the concept of the intermediate reference orbit for obtaining a first-order solution by analytical integration. The averaged equations of variation for zonal harmonics up to the fourth order are included. The literal expansions, partial differentiations, and integrations are carried out by a computerized series expansion technique employed by the author in studying the motion of the Galilean satellites[9]. The package of series expansion software used in this analysis is the latest version designed for the CDC 7600 computers by Broucke[10]. Although similar work has been done by Estes, the author considers it necessary to carry out the expansion and integration of this particular application for two reasons. With the help of computerized expansion it would take less effort and be more convenient to start from the averaged disturbing function developed by Kaufman than to use the analytical solutions published by Estes. Furthermore, Estes uses Brown's lunar theory for the motion of the moon which carries a great number of terms and is deemed to be unnecessary for this application. In this study, an earth equatorial coordinate system is used with orbit elements of the moon projected into this system using spherical trigonometry. For time spans of less than three years, a mean inclination and nodal rate interpolated from the true variation have been found to be good approximations for the analytical integration.

The rest of this paper is divided into two parts. Part I describes the theoretical formulation of the first-order solution and compares the long-term variations of the orbit elements of the GPS satellites predicted by the analytical solution with numerical integration. Part II presents an application of the first-order theory for the desired strategy of the orbit maintenance of the GPS satellites. Results of the investigation of long-term orbit perturbations of the GPS Phase III system are discussed.

## PART I: THEORETICAL FORMULATION

### Averaged Variational Equations

The disturbing function due to the third-body perturbation may be given in the earth-centered coordinates as

$$R' = \frac{\mu}{r'}\left[\left(1 + \frac{r^2}{r'^2} - \frac{2r}{r'}\cos S\right)^{-1/2} - \frac{r\cos S}{r'}\right] \qquad (1)$$

with

$\mu$ = gravitational constant ($k^2 m'$)

$r'$ = distance to the third body (sun/moon)

$r$ = distance to the satellite

$S$ = angle between the two position vectors, $\vec{r}$ and $\vec{r}'$

For the sun-moon perturbations of artificial earth satellites, we note that $r/r' \ll 1$. Therefore, we may expand the square root term in the above equation and neglect all terms of order $(r/r')^3$ and higher. Kaufman[6] has carried out the expansion and applied the method of averaging to eliminate the short-period terms. The resulting disturbing function is considerably simpler.

$$R' = \frac{a^2 n'^2}{2}\left(\frac{a'}{r'}\right)^3\left\{\left[\frac{3}{2}(A^2 + B^2) - 1\right]\left(1 + \frac{3e^2}{2}\right) + \frac{3}{2}(A^2 - B^2)\frac{5e^2}{2}\right\} \qquad (2)$$

with

$A = \vec{P} \cdot \vec{u}'$

$B = \vec{Q} \cdot \vec{u}'$

where $a$, $e$, $\vec{P}$, and $\vec{Q}$ are orbit parameters of the perturbed body and $a'$, $n'$, $r'$, and $\vec{u}'$ are parameters associated with the perturbing (third) body. The $\vec{u}'$ is the unit vector of the position of the third body.

Kaufman numerically integrated the variational equations of classical elements derived from the above disturbing function in terms of A and B; he then demonstrated that his method had a 500:1 increase of speed over an n-body numerical integration scheme. Although his method is fast and reasonably accurate, it does not give the analytical expressions which are important for analyzing and identifying the long-period terms of the perturbations.

The purpose of this paper is to further expand the disturbing function in terms of classical elements; thus, the variational equations (or perturbed equations) can be obtained by partial differentiation. With the assistance of a computerized series expansion technique, we can expand

the parameters $(A^2 + B^2)$ and $(A^2 - B^2)$ in the disturbing function of Eq. (2). The unit vectors $\vec{P}$, $\vec{Q}$, and $\vec{u}'$ may be written in terms of the classical elements (Fig. 1) as

$$\vec{P} = \begin{cases} \cos\Omega\cos\omega - \sin\Omega\sin\omega\cos i \\ \sin\Omega\cos\omega + \cos\Omega\sin\omega\cos i \\ \sin i\sin\omega \end{cases}$$

$$\vec{Q} = \begin{cases} -\sin\omega\cos\Omega - \cos\omega\sin\Omega\cos i \\ -\sin\omega\sin\Omega + \cos\omega\cos\Omega\cos i \\ \sin i\cos\omega \end{cases} \qquad (3)$$

and

$$\vec{u}' = \begin{cases} \cos\Omega'\cos u - \sin\Omega'\sin u\cos i' \\ \sin\Omega'\cos u + \cos\Omega'\sin u\cos i' \\ \sin i'\sin u \end{cases} \qquad (4)$$

where u is the argument of latitude of the third body.

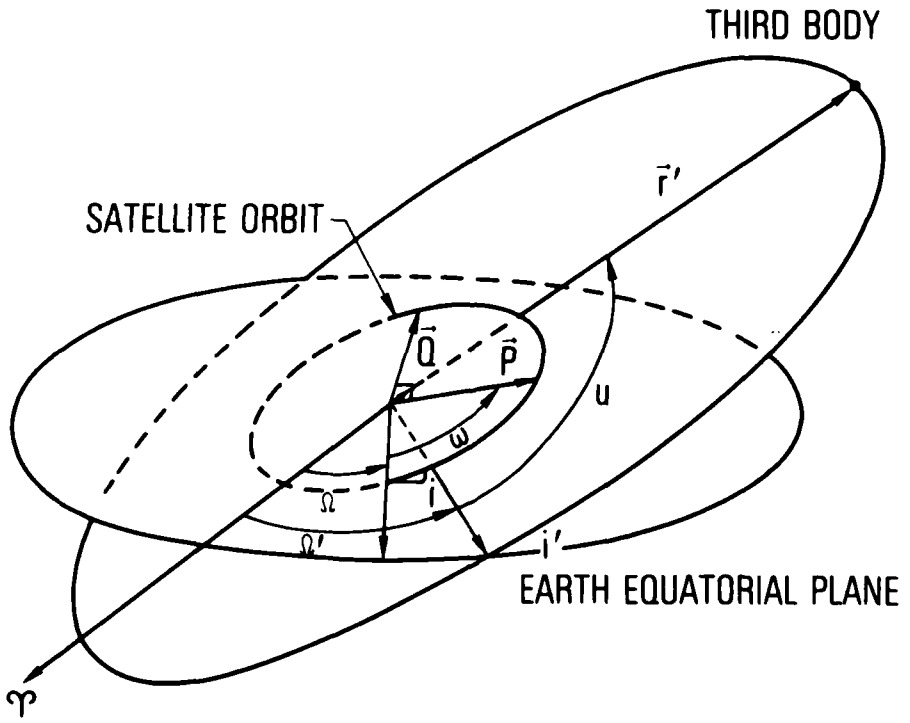


Fig. 1 Earth-Centered Geometry

We can express A and B in terms of the angles as

$$
\begin{aligned}
A = \vec{P} \cdot \vec{u}' &= \cos\omega(\cos u \cos\Delta\Omega + \cos i' \sin u \sin\Delta\Omega) \\
&\quad - \sin\omega \cos i \,(\cos u \sin\Delta\Omega - \sin u \cos\Delta\Omega \cos i') \\
&\quad + \sin i \sin i' \sin\omega \sin u \\
B = \vec{Q} \cdot \vec{u}' &= -\sin\omega\,(\cos u \cos\Delta\Omega + \sin u \sin\Delta\Omega \cos i') \\
&\quad - \cos\omega \cos i \,(\cos u \sin\Delta\Omega - \sin u \cos\Delta\Omega \cos i') \\
&\quad + \sin i \sin i' \cos\omega \sin u \qquad (5)
\end{aligned}
$$

where $\Delta\Omega = \Omega - \Omega'$.

In this first-order analysis, we assume that the third-body orbit is circular because of the small eccentricities of the orbits of the sun and moon. The series expansions may start from A and B using the computerized series expansion package. Each term of the series may be expressed in a general form as

$$
\text{Term} = C^{J_1..J_3}_{I_1..I_4} (SI)^{I_1} (CI)^{I_2} (SI3)^{I_3} (CI3)^{I_4} \begin{Bmatrix} \sin \\ \cos \end{Bmatrix} (J_1 L + J_2 W + J_3 D) \qquad (6)
$$

where

$$
C^{J_1..J_3}_{I_1..I_4} = \text{coefficient of each term}
$$

and

$$
\text{Polynomial Variables} \begin{cases} SI = \sin i \\ CI = \cos i \\ SI3 = \sin i' \\ CI3 = \cos i' \end{cases} \qquad \text{Angular Variables} \begin{cases} L = u \\ W = \omega \\ D = \Delta\Omega = \Omega - \Omega' \end{cases}
$$

The two series $(A^2 + B^2)$ and $(A^2 - B^2)$ in the averaged disturbing function Eq. (2), and other intermediate series, are expanded in literal form and printed out by a CDC 7600 computer at The Aerospace Corporation as shown in Appendix A, Table A-1. The variations of the classical elements of the perturbed body (an artificial satellite) may then be expressed in terms of the intermediate results shown in Appendix A.

$$\frac{da}{dt} = 0$$

$$\frac{de}{dt} = -\frac{15}{8} e\gamma s \,(IMW)$$

$$\frac{di}{dt} = -\frac{3}{4} \frac{\gamma \csc i}{s} \left[\left(1 + \frac{3}{2} e^2\right) IPO + \frac{5}{2} e^2 \,(IMO - \cos i \, IMW)\right]$$

$$\frac{d\Omega}{dt} = \frac{3}{4} \frac{\gamma}{s} \left[\left(1 + \frac{3}{2} e^2\right)\left(\frac{\cos i}{\sin i} IPS - IPC\right) + \frac{5}{2} e^2 \left(\frac{\cos i}{\sin i} IMS - IMC\right)\right]$$

$$\frac{d\omega}{dt} = \frac{3}{2} s\gamma \left[\frac{3}{2} (A^2 + B^2) - 1 + \frac{5}{2} (A^2 - B^2)\right] - \cos i \frac{d\Omega}{dt}$$

$$\frac{dM}{dt} = n - 2\gamma \left\{\left(1 + \frac{3}{2} e^2\right)\left[\frac{3}{2} (A^2 + B^2) - 1\right] + \frac{15}{4} e^2 (A^2 - B^2)\right\}$$
$$- \frac{3}{2} s^2 \gamma \left[\frac{3}{2} (A^2 + B^2) - 1 + \frac{5}{2} (A^2 - B^2)\right] \qquad (7)$$

where IMW, IMO, etc., are the intermediate series shown in Appendix A, and

$$\gamma = \frac{n'^2}{n} \left(\frac{a'}{r'}\right)^3 Rm$$

$$s = \sqrt{1 - e^2}$$

n = mean motion of the perturbed body

n' = mean motion of the perturbing body

Rm = mass ratio, Rm = 1 for solar perturbation and
Rm = 1/81.3 for lunar perturbation

Those important terms which give long-period and secular variations of classical elements due to third-body perturbations may be clearly seen from the above equations. The averaged variational equations for $J_2$, $J_3$, and $J_4$ can be found in Ref. 5; they are included in Appendix B for completeness.

Perturbations due to atmospheric drag and solar radiation pressure are not considered herein because of their insignificant effects on very long-period variations for higher-altitude satellites. The effect due to tesseral harmonics ($J_{22}$ to $J_{44}$, etc.) becomes important only when the mean motion of the satellite and the earth rotation rate are

commensurable. This effect will be included in Part II when this first-order theory is applied to the prediction of the longitude of the ascending node of the nearly 12-hr orbit of GPS satellites.

Analytical Integration

Those equations of variation expanded in series shown in the previous section may be integrated analytically to yield a first-order solution if the proper rates of the angular variables are known. The concept of an intermediate reference orbit or rotating ellipse allows us to have non-zero rates for the Keplerian angular elements $\Omega$ and $\omega$. The rates are calculated from the secular terms in the equations of variation. They may be summed up as

$$\dot{\Omega}_s = \dot{\Omega}_{sun} + \dot{\Omega}_{moon} + \dot{\Omega}_{J_2} + \dot{\Omega}_{J_4}$$

$$\dot{\omega}_s = \dot{\omega}_{sun} + \dot{\omega}_{moon} + \dot{\omega}_{J_2} + \dot{\omega}_{J_4} \qquad (8)$$

The secular terms, by definition, are those terms containing only the mean motion, eccentricity, and inclination which vary much more slowly than the node and argument or perigee. Those terms can be identified from the series, and they are

$$\dot{\Omega}_{sun} = -\frac{3}{8}\frac{n'^2}{n}\frac{\left(1+\frac{3}{2}e^2\right)}{\sqrt{1-e^2}}\cos i\,(3\cos^2 i' - 1) \qquad (9)$$

$$\dot{\omega}_{sun} = \frac{3}{4}\frac{n'^2}{n}\frac{\left(1-\frac{3}{2}\sin^2 i'\right)}{\sqrt{1-e^2}}\left(2-\frac{5}{2}\sin^2 i+\frac{e^2}{2}\right) \qquad (10)$$

When the third body is the moon, the above equations should be divided by the earth-moon mass ratio (81.3). The above expressions agree with those derived by Kozai[4]. The rates due to $J_2$ and $J_4$ are the secular part (terms without the argument $\omega$) of Eqs. (B-1) and (B-3).

$$\dot{\Omega}_{J_2} = -\frac{3}{2}n\epsilon_2\cos i - \frac{9}{4}n\epsilon_2^2\cos i\left[\frac{3}{2}-\frac{5}{6}\sin^2 i+\left(\frac{1}{6}+\frac{5}{24}\sin^2 i\right)e^2\right]$$

$$\dot{\omega}_{J_2} = \frac{3}{2}n\epsilon_2\left(2-\frac{5}{2}\sin^2 i\right) - \frac{9}{4}n\epsilon_2^2\left[2-\frac{23}{4}\sin^2 i+\frac{55}{16}\sin^4 i + \frac{e^2}{4}\left(7-\frac{9}{2}\sin^2 i+\frac{75}{4}\sin^4 i\right)\right]$$

$$\dot{\Omega}_{J_4} = n\epsilon_4\cos i\,[\,2(7\cos^2 i - 3) + e^2(21\cos^2 i - 9)] \qquad (11)$$

(cont.)

$$\dot{\omega}_{J_4} = -2n\epsilon_4 \left[ 8 - 28 \sin^2 i + 21 \sin^4 i - \frac{1}{2} \sin^2 i \,(7 \cos^2 i - 1) + e^2 \left( \frac{63}{8} - \frac{399}{16} \sin^2 i + \frac{567}{32} \sin^4 i \right) \right] \tag{11}$$

The mean motions n' of the sun and moon are known, and the integration is performed on the variations with secular terms removed. The integrated results for each perturbation ($J_2$, sun, etc.) may be expressed in a series form similar to Eq. (6).

$$\delta \begin{Bmatrix} e \\ i \\ \omega \\ \Omega \end{Bmatrix} = \sum_{\substack{I_i=0 \\ J_i=0}}^{N} \frac{C_{I_1 \cdots I_5}^{J_1 \cdots J_3} SI^{I_1} CI^{I_2} SI3^{I_3} CI3^{I_4} e^{I_5}}{J_1 n' + J_2 \dot{\omega}_s + J_3 (\dot{\Omega}_s - \dot{\Omega}'_s)} \left[ \begin{Bmatrix} \sin \\ \cos \end{Bmatrix} \left( J_1 L + J_2 W + J_3 D \right) - \begin{Bmatrix} \sin \\ \cos \end{Bmatrix} \left( J_1 L_0 + J_2 W_0 + J_3 D_0 \right) \right] \tag{12}$$

where

$$L = n'(t-t_0) + L_0$$

$$W = \dot{\omega}_s (t-t_0) + W_0$$

$$D = (\dot{\Omega}_s - \dot{\Omega}'_s)(t-t_0) + D_0$$

and

$L_0$ = argument of latitude of the perturbing body at $t_0$

$W_0$ = argument of perigee of the perturbing body at $t_0$

$D_0$ = the value of $(\Omega - \Omega')$ at $t_0$

The values of inclination and eccentricity of the perturbed body or the satellite at the epoch time $t_0$ are substituted into the polynomial variables SI, CI.... in Eq. (12). The inclination of the sun, i', is nothing but the inclination of the ecliptic plane.

The inclination i', argument of latitude L, right ascension of the node $\Omega'$, and rate $\dot{\Omega}'$ of the moon must be computed in a special way because of the earth equatorial coordinate system. From Fig. 2 and the relations of spherical trigonometry, we have elements for the moon referred to the earth equatorial system as

$$i' = \cos^{-1}\left[\cos\epsilon \cos i_e - \sin\epsilon \sin i_e \cos\Omega_e\right]$$

$$\Omega' = \sin^{-1}\left[\frac{\sin i_e \sin\Omega_e}{\sin i'}\right]$$

$$L = u_e + \Delta u_e$$

$$\Delta u_e = \sin^{-1}\left[\frac{\sin\Omega_e \sin\epsilon}{\sin i'}\right] \tag{13}$$

$$\dot{\Omega}' = \frac{\sin i_e}{\sin i'}\left[\frac{\cos\Omega_e}{\cos\Omega'} + \frac{\sin^2\Omega_e \sin\epsilon \sin i_e}{\cos\Omega' \sin i' \tan i'}\right]\dot{\Omega}_e \tag{14}$$

where quantities with a subscript e are referred to the ecliptic system. The equations of $\Omega_e$, $u_e$, and $i_e$ are found in the American Ephemeris.* If we limit the time span of interest to a couple of years, a mean inclination and nodal rate interpolated from the true variations shown by Fig. 3 should give a good approximation for the integration. This approximation is particularly good during the interval from about 1984 to 1992, where the variations in inclination and nodal rate are relatively small.

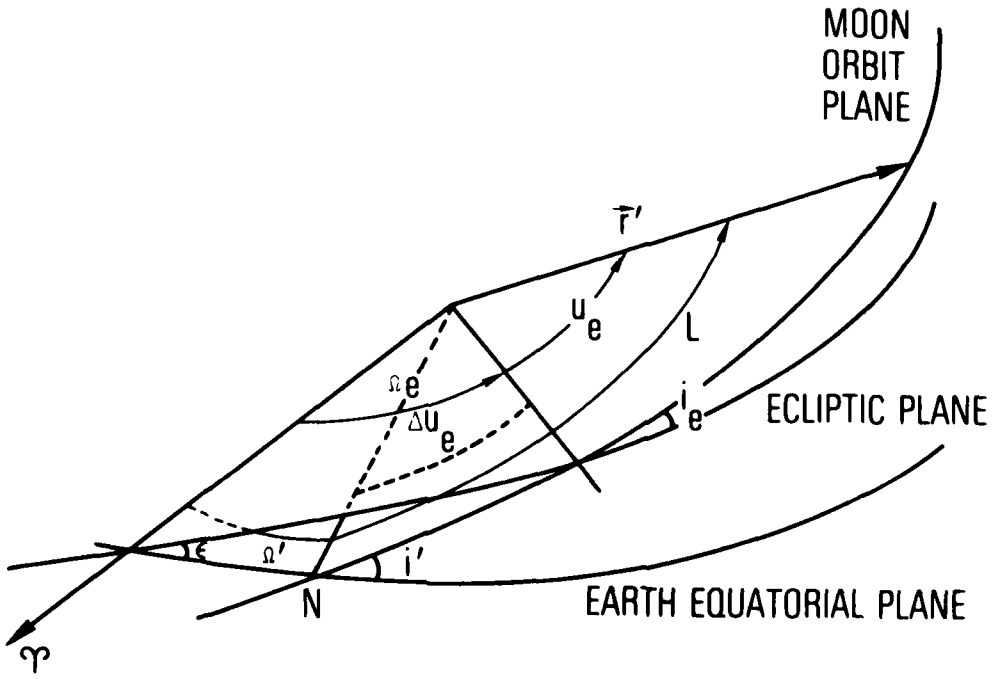


Fig. 2 Geometry of Orbit Planes

*American Ephemeris and Nautical Almanac, published by the U.S. Naval Observatory.

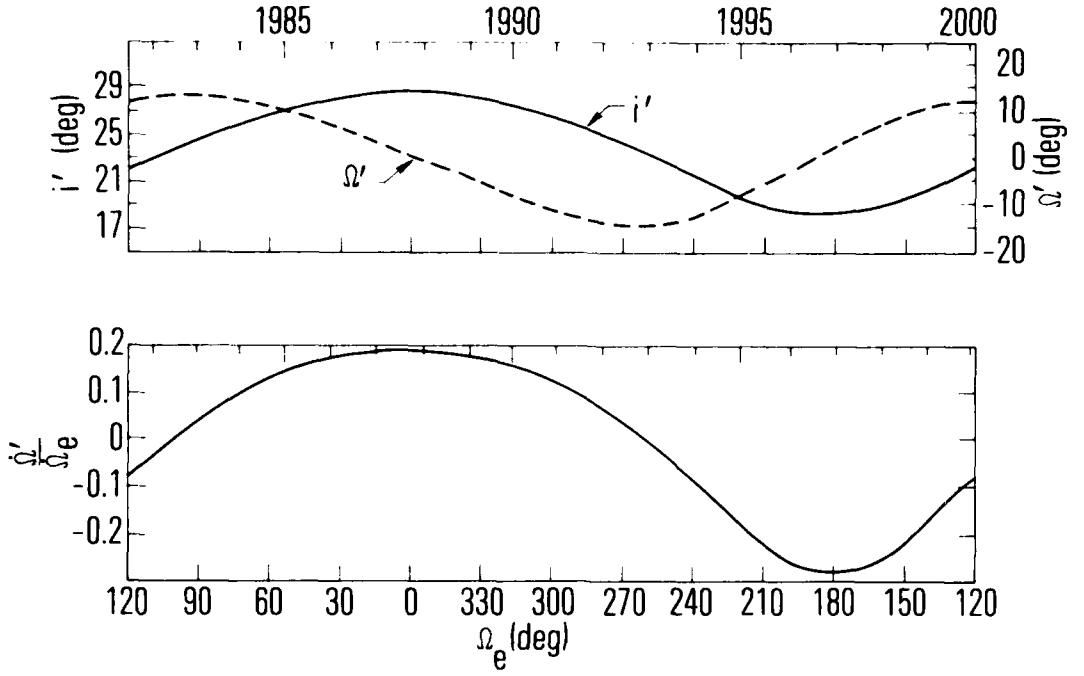


Fig. 3 Variations of Inclination and Node of the Moon in Earth Equatorial Coordinates

Finally, the first-order solution is the linear combination of the integrated variational equations due to each perturbation.

$$\delta\begin{Bmatrix} e \\ i \\ \Omega \\ \omega \end{Bmatrix} = \delta\begin{Bmatrix} e \\ i \\ \Omega \\ \omega \end{Bmatrix}_{J_2} + \delta\begin{Bmatrix} e \\ i \\ \Omega \\ \omega \end{Bmatrix}_{J_3} + \delta\begin{Bmatrix} e \\ i \\ \Omega \\ \omega \end{Bmatrix}_{J_4} + \delta\begin{Bmatrix} e \\ i \\ \Omega \\ \omega \end{Bmatrix}_{sun} + \delta\begin{Bmatrix} e \\ i \\ \Omega \\ \omega \end{Bmatrix}_{moon} + \begin{Bmatrix} 0 \\ 0 \\ \dot{\Omega}_s \\ \dot{\omega}_s \end{Bmatrix}(t-t_o) \tag{15}$$

Comparisons with Numerical Integration

Orbit variations in terms of Keplerian elements are calculated from the first-order solution for a span of 800 days. The initial conditions at a common epoch of 1 July 1985 at 0 hr are listed below.

$$a = 14341.8 \text{ nmi}, \quad e = \begin{Bmatrix} 0.01 \\ 0.7 \end{Bmatrix}, \quad i = \begin{Bmatrix} 5 \text{ deg} \\ 30 \text{ deg} \\ 63 \text{ deg} \end{Bmatrix}, \quad \Omega = 40 \text{ deg},$$

$$\omega = 60 \text{ deg}, \quad M = 0 \text{ deg}$$

Results of these six different cases are compared with the results computed by the program ELEMENT, developed by B. Baxter of The Aerospace Corporation[11], which numerically integrate the singly averaged equations of variation shown above in "Analytical Integration." The same perturbative model including $J_2$ through $J_4$, the sun, and the moon is used in the numerical integration. The comparison indicates that the variations in eccentricity and inclination predicted by the first-order solution agree amazingly well with that generated by ELEMENT for low-eccentricity orbits as shown by Figs. 4, 5, 7, 8, and 9. The discontinuity in slope in the curves of numerical integration is simply caused by the rather large step size in plotting. For high-eccentricity orbits, the agreement is generally good up to 400 days as shown by Figs. 6 through 9. After 400 days, the prediction by the analytical solution is noticeably different from the true variation.

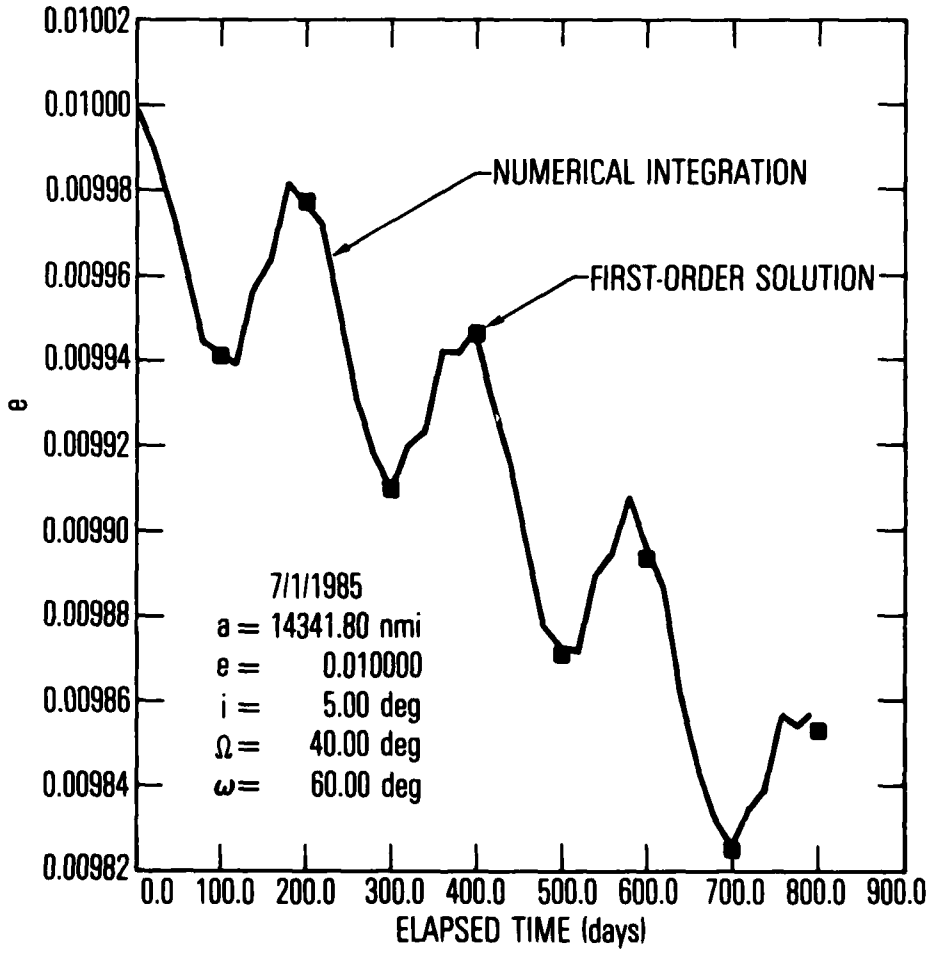


Fig. 4 Eccentricity Time History for Low Inclination Orbit (i = 5 deg)

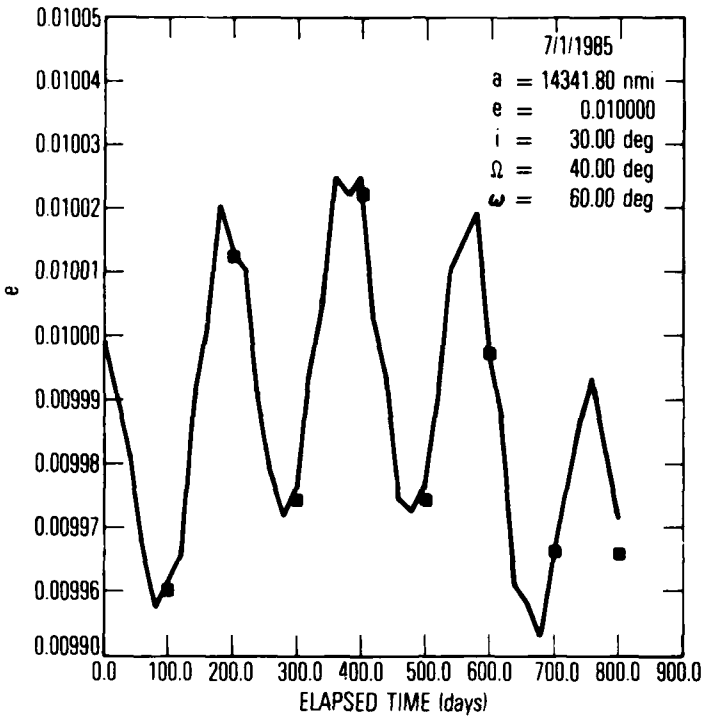


Fig. 5 Eccentricity Time History for Moderate Inclination Orbit (i = 30 deg)

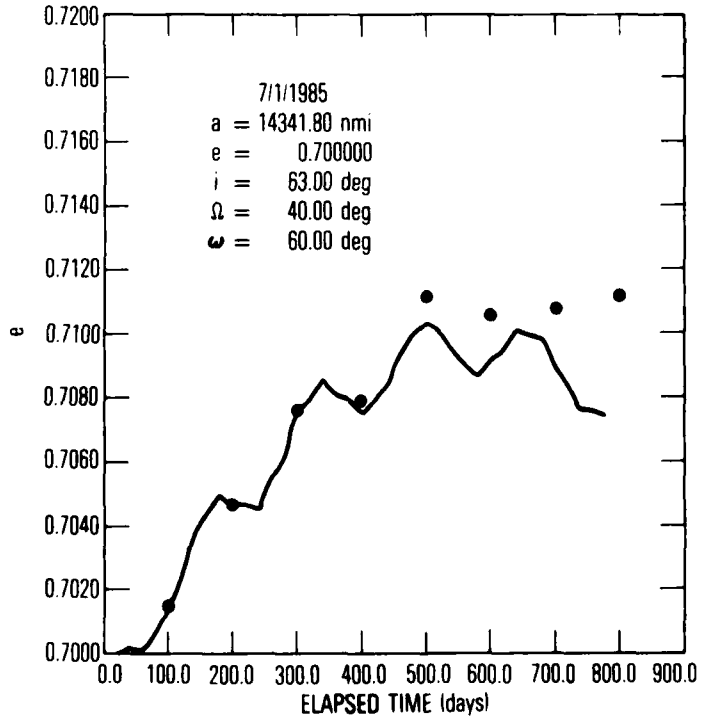


Fig. 6 Eccentricity Time History for High Eccentricity Orbit (i = 63 deg)

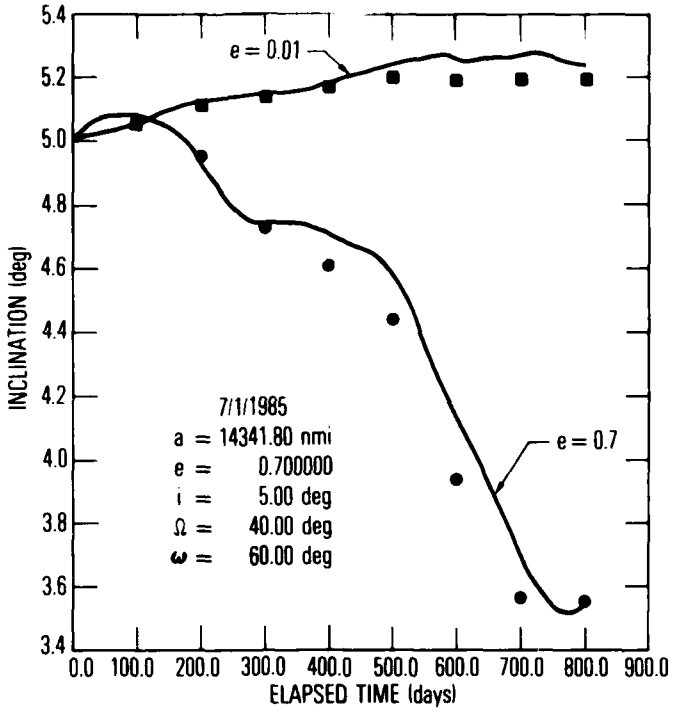


Fig. 7 Inclination Time History for Low Inclination Orbit (i = 5 deg)

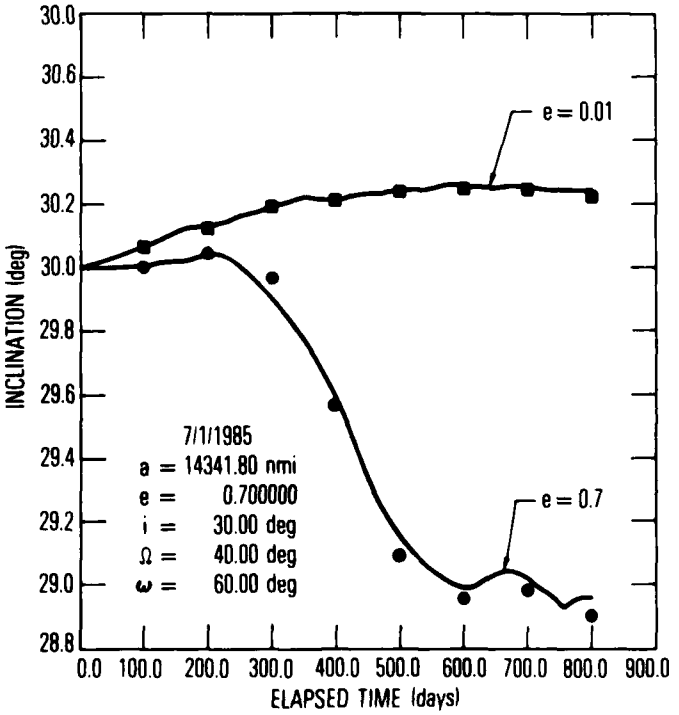


Fig. 8 Inclination History for Moderate Inclination Orbit (i = 30 deg)

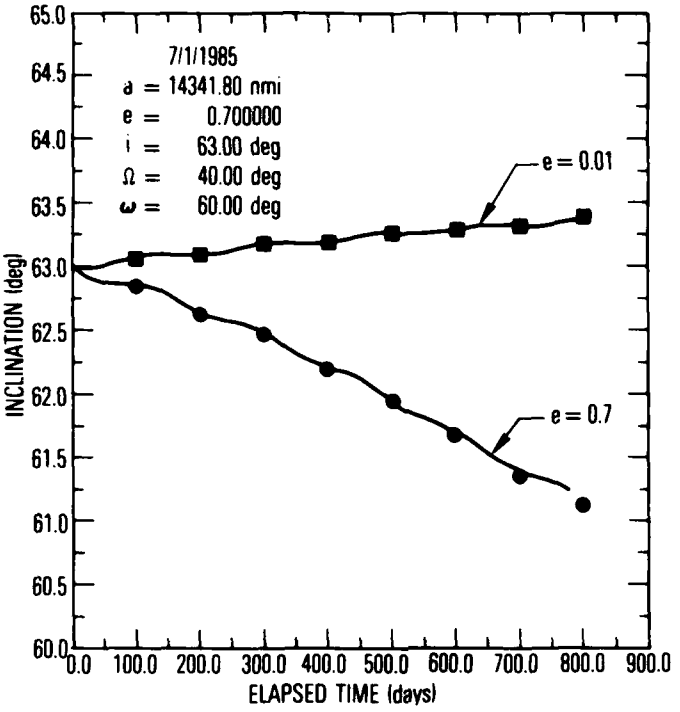


Fig. 9 Inclination Time History for High Inclination Orbit (i = 63 deg)

This is probably because of the relatively large variations in the mean orbit elements due to the high eccentricity. Nevertheless, the general trend of variation in the 800-day span has been predicted by the first-order solution. Table 1 shows the comparison for other orbit elements $\Omega$ and $\omega$ that are not shown in Figs. 4 through 9. Table 2 shows the comparison for a GPS satellite with a = 14341.8, e = 0.005, i = 45 deg, $\Omega$ = 265.4553 deg, and $\omega$ = 90 deg.

The accuracy of the first-order solution may be improved slightly by including the eccentricity of the orbits of the sun and moon. The series expansion for such an inclusion was made; it is found that even to the first order in eccentricity e', the total number of terms in the disturbing function as well as in the equations of variation has increased nearly three times! The penalty in computing time and complexity would be too great for a small improvement in accuracy. Therefore, we did not make the comparison with numerical integration.

Table 1

## DIFFERENCES BETWEEN FIRST-ORDER SOLUTION AND NUMERICAL INTEGRATION*

| Days from Epoch | e = 0.01 | | | | | | e = 0.7 | | | | | |
|---|---|---|---|---|---|---|---|---|---|---|---|---|
| | $\Delta\Omega$** | | | $\Delta\omega$ | | | $\Delta\Omega$ | | | $\Delta\omega$ | | |
| | i = 5 | i = 30 | i = 63 | i = 5 | i = 30 | i = 63 | i = 5 | i = 30 | i = 63 | i = 5 | i = 30 | i = 63 |
| 100 | 0.021 | -0.018 | -0.014 | 0.003 | 0.049 | 0.013 | -1.492 | -0.301 | 0.099 | 1.799 | 0.443 | -0.121 |
| 200 | 0.037 | -0.038 | -0.030 | 0.010 | 0.107 | 0.037 | -3.300 | -0.670 | 0.520 | 4.202 | 0.979 | -0.391 |
| 300 | 0.091 | -0.059 | -0.054 | -0.014 | 0.185 | 0.085 | -4.440 | -0.987 | 1.105 | 5.714 | 1.382 | -0.850 |
| 400 | 0.199 | -0.087 | -0.087 | -0.078 | 0.293 | 0.146 | -5.784 | -1.339 | 2.043 | 7.804 | 1.729 | -1.573 |
| 500 | 0.242 | -0.112 | -0.117 | -0.123 | 0.358 | 0.214 | -6.900 | -1.215 | 3.135 | 9.695 | 1.161 | -2.514 |
| 600 | 0.318 | -0.137 | -0.152 | -0.181 | 0.444 | 0.299 | -9.840 | -1.366 | 4.398 | 12.626 | 0.912 | -3.758 |
| 700 | 0.397 | -0.166 | -0.199 | -0.217 | 0.567 | 0.405 | -10.750 | -1.663 | 5.838 | 13.765 | 0.829 | -5.293 |
| 800 | 0.383 | -0.190 | -0.242 | -0.133 | 0.680 | 0.466 | -6.786 | -2.528 | 7.073 | 9.722 | 1.530 | -6.919 |

*Units: angles in deg

**$\Delta\Omega$, $\Delta\omega$ = (first-order theory)-(numerical integration)

Table 2

DIFFERENCE BETWEEN FIRST-ORDER THEORY AND NUMERICAL INTEGRATION

| Days from Epoch | e x10$^{-4}$ | | i (deg) | | $\Omega$ (deg) | | $\omega$ (deg) | |
|---|---|---|---|---|---|---|---|---|
| | N.I.* | $\Delta$e** | N.I.* | $\Delta$i | N.I.* | $\Delta\Omega$ | N.I.* | $\Delta\omega$ |
| 100 | 49.73 | 0.02 | 44.899 | -0.002 | 260.48 | -0.01 | 91.95 | -0.027 |
| 200 | 49.04 | 0.15 | 44.827 | -0.002 | 255.55 | -0.01 | 93.79 | -0.027 |
| 300 | 48.43 | 0.35 | 44.780 | -0.003 | 250.54 | -0.004 | 95.85 | -0.022 |
| 400 | 47.66 | 0.59 | 44.678 | -0.004 | 245.63 | -0.003 | 97.55 | 0.033 |
| 500 | 46.77 | 0.92 | 44.661 | -0.004 | 240.65 | 0.03 | 99.56 | 0.109 |
| 600 | 45.90 | 1.31 | 44.567 | -0.003 | 235.71 | 0.05 | 101.24 | 0.24 |
| 700 | 44.74 | 1.7 | 44.547 | -0.004 | 230.78 | 00.08 | 103.05 | 0.45 |
| 800 | 43.77 | 2.3 | 44.480 | -0.001 | 225.81 | 0.10 | 104.71 | 0.69 |

*N.I. = numerical integration of the averaged equations

**$\Delta$e, $\Delta$i... = (first-order theory) - (numerical integration)

## PART II: APPLICATION

### Background

The particular application, presented in detail below, is for the desired strategy of orbit maintenance. During the mission design of the GPS orbits, a family of orbits was numerically integrated with the averaged equations[8] to study the long-term characteristics. For each orbit a series of impulses or orbit corrections must be simulated during the integration so that the longitude of the ascending node crossing remains within a specified tolerance ($\pm$1 deg) for repeating ground track coverage. The GPS satellites have a nearly 12-hr period, and are required to have repeating ground tracks every two revolutions at a specified longitude of the ascending node crossing. The initial conditions are determined in such a manner as to synchronize the repeating ground track in the presence of perturbations. However, as time goes on, the perturbations due to the earth gravitational potential ($J_2, \ldots J_4$, $J_{2\,2} \ldots J_{4\,4}$), the sun, and the moon drive the longitude of the node away from the specified value.

The method of orbit maintenance developed in Ref. 12 makes use of the scalloping motion depicted in Fig. 11. The perturbation in semi-major axis provides the restoring acceleration for a longitude drift

induced by a $\Delta V$ perturbation. The method functions open loop, however, by utilizing the induced drift rate for the first correction in all subsequent corrections. This leads to difficulties if the perturbations in argument of perigee and right ascension of ascending node begin to dominate the perturbation in semimajor axis as happens for certain of the GPS orbits. The open-loop technique also fails to completely fill the dead band even though the perturbed state, together with the conditions of repeatability, is used to calculate each $\Delta V$. This arises because the $\Delta V$ is not adjusted by observing the depth of the scallop.

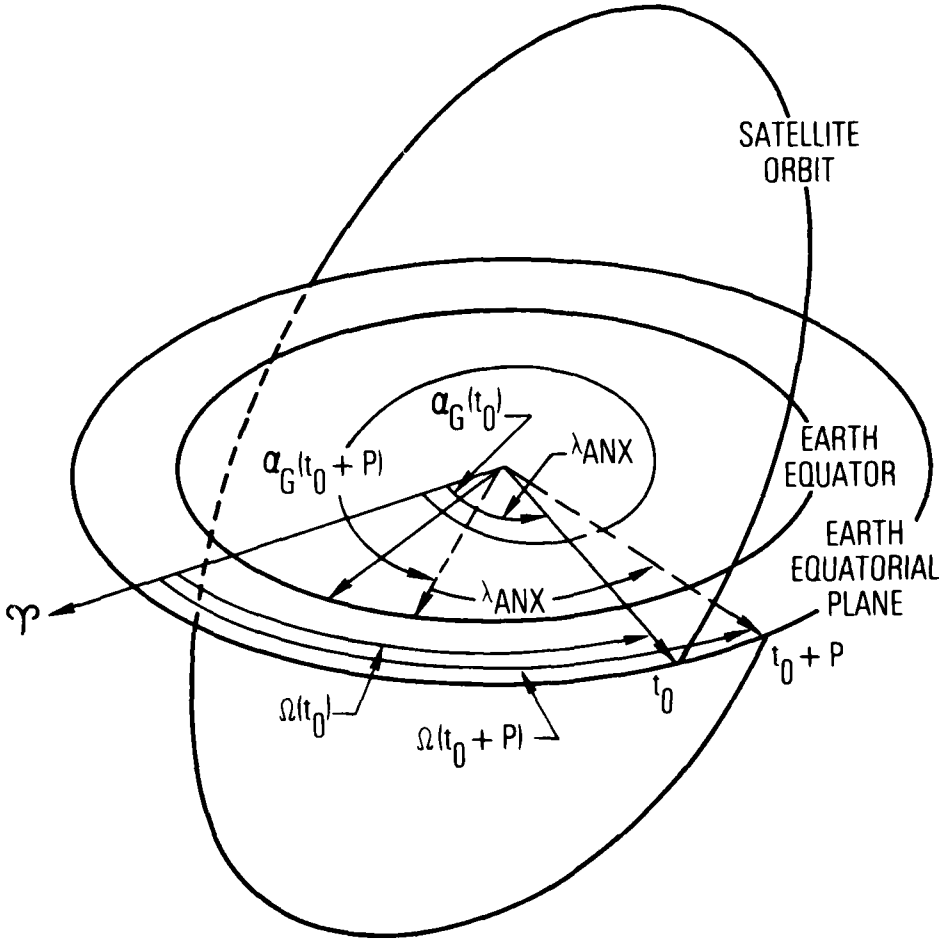


Fig. 10 Orbit Geometry for Repeating Ground Track Coverage (Q = 1 orbit)

An algorithm which applies the first-order theory for longitude prediction, which in turn provides the desired strategy for orbit maintenance, has been developed and employed for simulating the orbit corrections during the integration of the 24 orbits of the GPS Phase III system.

Analysis

Let us begin with the earth equatorial system in inertial space. Figure 10 illustrates the orbit geometry. For repeating ground track coverages, we require that the longitude (earth-fixed) of the ascending node crossing of the satellite, $\lambda_{ANX}$, repeats every Q revolutions, or

$$\alpha_G(t_0 + NP) + \lambda_{ANX} = \Omega(t_0 + NP) + \frac{2N\pi}{Q} \qquad (16)$$

with

N = 0, 1, 2.....

$t_0$ = epoch time when the ascending node crossing occurs at longitude $\lambda_{ANX}$

P = nodal period

$\alpha_G$ = right ascension of Greenwich

$\Omega$ = right ascension of the ascending node

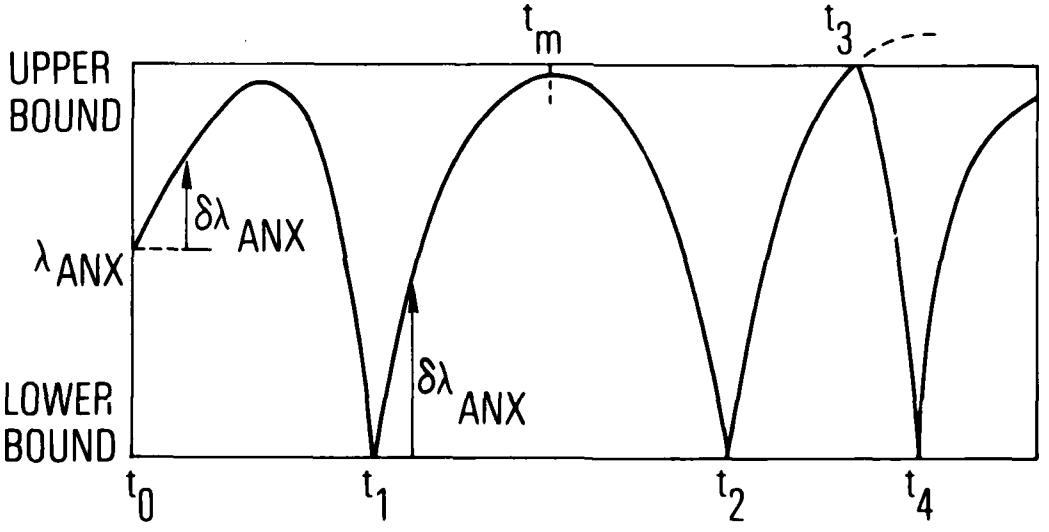


Fig. 11 Schematic Drawing of the Time History of Orbit Corrections

Assuming a constant earth rotation rate and a constant nodal regression rate determined from the perturbations due to $J_2$, etc., at $t_0$, we can rewrite the above equation as

$$a_G(t_0) + NP\,\dot{a}_G + \lambda_{ANX} = \Omega(t_0) + \dot{\Omega}(t_0)\,NP + \frac{2\pi N}{Q} \tag{17}$$

As time goes on, the nodal period P and the nodal regression rate $\dot{\Omega}$ vary due to perturbations; consequently, $\lambda_{ANX}$ slowly drifts away from the original value. By varying Eq. (17), we obtain the variation in $\lambda_{ANX}$ as a function of the variations in P and $\Omega$ as

$$\delta\lambda_{ANX} = [\dot{\Omega}(t_0) - \dot{a}_G]\,\delta(NP) + \delta\dot{\Omega}NP \tag{18}$$

Since $\delta\dot{\Omega}$ is not constant, the nodal variation should actually be

$$\delta\dot{\Omega}NP = \int_{t_0}^{t_0+NP} [\dot{\Omega}(t) - \dot{\Omega}(t_0)]dt \tag{19}$$

The term $\delta(NP)$ is defined as the variation in time measured in accumulated variations of nodal periods since the epoch $t_0$. It may be expressed as follows:

$$\delta(NP) = \int_{t_0}^{t_0+NP} \frac{\delta P}{P}\,dt \tag{20}$$

where $\delta P/P$ is the variation in period per one nodal period, which may be related to the variations of the mean classical elements through the following derivation.

Let

$$P = \frac{2\pi}{\dot{\bar{u}}} \tag{21}$$

then

$$\frac{\delta P}{P} = -\frac{\delta\dot{\bar{u}}}{\dot{\bar{u}}} \tag{22}$$

where $\dot{\bar{u}}$ is the mean angular rate of the argument of latitude in the perturbed orbit. It has two components

$$\dot{\bar{u}} = n + \dot{\bar{u}}' \tag{23}$$

The first is the classical component which is the mean motion of the orbit; the second component is the mean variation due to perturbations (as denoted by \ following Herrick[13]). We know from Ref. 13 (Chapters 15 and 17) that

$$\bar{u}^{\backslash} = -\Omega^{\backslash} \cos i = -\dot{\Omega} \cos i \tag{24}$$

where $\Omega^{\backslash}$ or $\dot{\Omega}$ is the mean (averaged over one period) nodal rate of the perturbed orbit. By varying Eqs. (23) and (24), we obtain to the first order that

$$\delta \dot{\bar{u}} = \delta n - \delta \dot{\Omega} \cos i \tag{25}$$

Substituting Eqs. (23) through (25) into Eq. (22), we have

$$\frac{\delta P}{P} = - \frac{\delta n - \delta \dot{\Omega} \cos i}{n - \dot{\Omega} \cos i} \tag{26}$$

where $\delta \dot{\Omega}$ is simply $\dot{\Omega}(t) - \dot{\Omega}(t_0)$, and the variation in the mean motion $\delta n$ derives from the variation in semimajor axis $\delta a$ as

$$\delta n = - \frac{3}{2} n \frac{\delta a}{a} \tag{27}$$

After combining Eqs. (26), (27), and (20), and substituting Eqs. (19) and (20) into Eq. (18), we obtain the relation between the longitude variation and the variations in the mean classical elements.

$$\delta \lambda_{ANX} = (1 - \beta \cos i) \int_{t_0}^{t_0+NP} [\dot{\Omega}(t) - \dot{\Omega}(t_0)] dt - \frac{3}{2} n \beta \int_{t_0}^{t_0+NP} \frac{\delta a}{a} dt \tag{28}$$

where

$$\beta = \frac{\dot{a}_G - \dot{\Omega}(t_0)}{n - \dot{\Omega}(t_0) \cos i}$$

The averaged equations of variation of $\dot{\Omega}(t)$ are derived and listed in Part I of this paper. For satellites with mean motion commensurable with the earth's rotation rate, the effects due to tesseral harmonics must be included. The variations in semimajor axis are induced primarily by the tesseral harmonics. Therefore, terms with resonant angles must be carefully examined and integrated. Kaula[14] provided a set of integrated equations in a general form for perturbations due to tesseral harmonics. For the 12-hr (Q=2) orbits, we include $J_{22}[(2, 2, 1, 1), (2, 2, 0, -1)]$, $J_{32}[(3, 2, 1, 0), (3, 2, 2, 2), (3, 2, 0, -2)]$, $J_{42}[(4, 2, 1, -1),$

(4, 2, 2, 1)], and $J_{44}[(4, 4, 1, 0), (4, 4, 0, -2)]$ as

$$\frac{\Delta a}{a} = n\sum\left[\left(\frac{ae}{a}\right)^{\ell} 2(\ell - 2p+q)\, F_{\ell mp}\, G_{\ell pq}\, C_{\ell mpq}\right]$$

$$\Delta\Omega = \frac{n}{\sqrt{1-e^2}\sin i}\sum\left[\left(\frac{ae}{a}\right)^{\ell}\left(\frac{\partial F_{\ell mp}}{\partial i}\right) G_{\ell pq}\, \overline{C}_{\ell mpq}\right] \quad (29)$$

where

$$C_{\ell mpq} = \sqrt{C_{\ell m}^2 + S_{\ell m}^2}\ \frac{\cos\left[(\ell-2p)\omega + (\ell-2p+q)M + m(\Omega - a_G) - \lambda_{\ell m}\right]}{(\ell-2p)\dot{\omega} + (\ell-2p+q)\dot{M} + m(\dot{\Omega} - \dot{a}_G)}$$

$$\overline{C}_{\ell mpq} = \sqrt{C_{\ell m}^2 + S_{\ell m}^2}\ \frac{\sin\left[(\ell-2p)\omega + (\ell-2p+q)M + m(\Omega - a_G) - \lambda_{\ell m}\right]}{(\ell-2p)\dot{\omega} + (\ell-2p+q)\dot{M} + m(\dot{\Omega} - \dot{a}_G)}$$

$\lambda_{\ell m} = \tan^{-1}\left(\frac{S_{\ell m}}{C_{\ell m}}\right)$ $\quad \ell$-m even

$\lambda_{\ell m} = \tan^{-1}\left(-\frac{C_{\ell m}}{S_{\ell m}}\right)$ $\quad \ell$-m odd

$M$ = mean anomaly of the satellite

The functions $F_{221}$, $G_{221}$, etc., are the inclination and eccentricity functions tabulated in Appendix C.

For orbits with periods of nearly 12 hr, the divisors in Eqs. (29) and (30) may become very small.

$$(\ell-2p)\dot{\omega} + \dot{M} + 2(\dot{\Omega} - \dot{a}_G) \approx 0 \quad (30)$$

Generally speaking, the first-order solutions [Eqs. (29)] usually break down in the vicinity of a resonance. Fortunately, the orbit maintenance corrections confine the value of $\dot{M}$ to within a small range for repeating ground tracks. Consequently, this stabilizes the small divisors and makes the first-order solution valid. In the event the divisor becomes smaller than the known angular rates $\dot{M}$, $\dot{\omega}$, and $\dot{\Omega}$ of the orbit ($\approx 2 \times 10^{-5}$ rad/day), the following approximation should be adequate for predicting the variations from about 200 to 400 days for orbit maintenance purposes.

$$\left(\frac{da}{dt}\right)_{J_{\ell m}} = \text{constant}\ , \quad \left(\frac{d\Omega}{dt}\right)_{J_{\ell m}} = \text{constant} \quad (31)$$

The right-hand side of the above equations can be obtained by differentiating Eqs. (29). The additional nodal rates from Eq. (31) should be added to the total nodal rate $\dot{\Omega}_s$ as shown in Eq. (8).

An Algorithm for Orbit Maintenance

The desired strategy of orbit maintenance is to keep to a minimum the number of corrections, i.e., impulses, within a given time span. In other words, the $\Delta V$ should be correctly determined so that the time interval between two adjacent corrections is a maximum without getting outside the specified range as shown by Fig. 10. For GPS satellites, the time interval between corrections varies from 200 to 400 days; it is too costly to numerically integrate the orbit from $t_1$ to $t_2$ (Fig. 11) in an iterative manner for the determination of $\Delta V$ at $t_1$. Thus, the first-order solution which predicts the longitude variation due to the effects of the sun, moon, and earth gravitational potential as shown by Eq. (28) is employed to determine the $\Delta V$ at each orbit correction.

After the integrations in Eq. (28) are performed, the longitude variation may be expressed in series form

$$\delta\lambda_{ANX} = \sum_{i=1}^{N} B_i \left[ \begin{Bmatrix} \sin \\ \cos \end{Bmatrix} [\gamma_i (t-t_j) + g_i] - \begin{Bmatrix} \sin \\ \cos \end{Bmatrix} (g_i) \right] \qquad (32)$$

where $\delta\lambda_{ANX}$ is the variation of longitude of ascending node from the epoch value at time $t_j$ when an orbit correction is made, and $B_i$, $\gamma_i$, and $g_i$ are constants computed from mean orbit elements i, e, n, and initial conditions.

As shown by Fig. 10, the first orbit correction should be made at $t_1$ when the value of $\lambda_{ANX}$ reaches the lower bound. The desired strategy requires that the maximum variation of $\delta\lambda_{ANX}$ occurs at $t_m$ (the restoring force is the tesseral harmonics) with its magnitude nearly equal to the specified tolerance, say 2 deg. Let $t_j$ be the time of an orbit correction and $t_m$ at some time between $t_j$ and $t_{j+1}$, which is the time of the next correction. We have

$$\delta\lambda_{ANX}(t_m) = 2 \text{ deg} = \sum_{i=1}^{N} B_i \left\{ \begin{pmatrix} \sin \\ \cos \end{pmatrix} [\gamma_i (t_m - t_j) + g_i] - \begin{pmatrix} \sin \\ \cos \end{pmatrix} (g_i) \right\}$$

$$+ \Delta\lambda_j (t_m - t_j) \qquad (33)$$

With the slope equal to zero at $t_m$, we require

$$\delta\dot{\lambda}_{ANX}(t_m) = \sum_{i=1}^{N} B_i \gamma_i \left\{ \begin{pmatrix} \cos \\ -\sin \end{pmatrix} [\gamma_i (t_m - t_j) + g_i] \right\} + \Delta\dot{\lambda}_j = 0 \qquad (34)$$

The second term on the right-hand side of the above equations is introduced when an orbit correction is made at $t_j$. The introduced constant rate $\Delta\dot{\lambda}_j$ at $t_j$ is an unknown parameter to be determined. With the above equations we should be able to determine the two unknowns $t_m$ and $\Delta\dot{\lambda}_j$. An interative formula derived from Newton's iteration method is constructed to compute $t_m$.

$$t_m = t_{m_0} - \frac{F(t_{m_0})}{F'(t_{m_0})} \qquad (35)$$

where

$$F(t_m) = \sum_{i=1}^{N} B_i \left[ \begin{Bmatrix} \sin \\ \cos \end{Bmatrix} \theta_i - \begin{Bmatrix} \sin \\ \cos \end{Bmatrix} g_i \mp \gamma_i (t_m - t_j) \begin{Bmatrix} \cos \\ \sin \end{Bmatrix} \theta_i \right] - \chi \delta\lambda_{bound}$$

$$F'(t_m) = \sum_{i=1}^{N} B_i \gamma_i^2 (t_m - t_j) \begin{Bmatrix} \sin \\ \cos \end{Bmatrix} \theta_i \qquad (36)$$

with

$$\theta_i = \gamma_i (t_m - t_j) + g_i$$

$\delta\lambda_{bound}$ = specified bound, 2 deg

The parameter $\chi$ is a factor which is slightly smaller than 1, so that the true variation will not exceed the specified bound $\delta\dot{\lambda}_{bound}$. Once $t_m$ is obtained after iteration, $\Delta\dot{\lambda}_j$ is determined from Eq. (34). By differentiating Eq. (28), we can determine the correction for semi-major axis from the value of $\Delta\dot{\lambda}_j$ as

$$\left(\frac{\Delta a}{a}\right)_{t_j} = \frac{2}{3} \frac{\Delta\dot{\lambda}_j}{n\beta} \qquad (37)$$

or a corresponding correction to the period of

$$\left(\frac{\Delta P}{P}\right)_{t_j} = \frac{\Delta \dot{\lambda}_j}{n\beta} \tag{38}$$

The initial guess of $t_{m_0}$ may be determined from an approximation that the small divisors in Eqs. (29) or (30) vanish and $\delta\dot{\Omega}$ is zero. Then

$$\frac{\dot{a}}{a} = \text{constant} = \epsilon \tag{39}$$

or

$$\frac{\delta a}{a} = \epsilon\,(t - t_j)$$

By satisfying the same conditions, Eqs. (33) and (34), we can solve for $t_{m_0}$ as

$$t_{m_0} = t_j + \sqrt{\frac{4\chi\,\delta\lambda_{bound}}{3\beta n\epsilon}} \tag{40}$$

Usually, the longitude of the ascending node crossing is sustained to the initial value within a dead band of ± 1 deg. The sustenance strategy functions by applying impulses at perigee when the longitude $\lambda_{ANX}$ violates a boundary of the dead band. The impulse is performed to adjust the period in order to give a repeating ground track at the time of the correction; that is, the synchronous period is redetermined to include the effect of perturbations in the elements and the predicted variation, using the new algorithm described above. The new semimajor axis is determined by the following relation:

$$\frac{2\pi}{\sqrt{\frac{\mu}{a^3}}} + \Delta P_1 + \Delta P_2 + \Delta P_3 = P_{required} \tag{41}$$

where

$a$ = new semimajor axis

$\Delta P_1$ = period variation predicted for optimum orbit sustenance (the new algorithm)

$P_{required} = 2\pi/\left(\dot{a}_G - \dot{\Omega}\right)$

and

$\dot{\alpha}_G$ = rate of the right ascension of Greenwich, $7.292115431 \times 10^{-5}$ rad/sec

$\dot{\Omega}$ = mean rate of the right ascension of the ascending node

The period variation due to $J_2$ effect, $\Delta P_2$, is obtained from Claus and Lubowe[15].

$$\frac{\Delta P_2}{P} = -\frac{3}{2} J_2 \left(\frac{a_e}{a}\right)^2 \left[\left(\frac{a}{r}\right)^3 + \frac{1}{2} \frac{1}{\sqrt{1-e^2}} \frac{4-5\sin^2 i}{(1+e\cos\omega)^2}\right] \quad (42)$$

with $a_e$ = earth equatorial radius, $r = a(1-e^2)/(1+e\cos\omega)$, and $P = 2\pi/\sqrt{\mu/a^3}$. The period variation due to the sun-moon perturbation is similarly derived as

$$\frac{\Delta P_3}{P} = \frac{3}{2\pi} \left(\frac{n'}{n}\right)^2 \left(\frac{a'}{r'}\right)^3 (1-e^2)^{9/2} \, Rm \cot i \, (xy' \, U1 + yy' \, U2) \quad (43)$$

where

$$Rm = \text{mass ratio} = \begin{matrix} 1\text{:solar perturbation} \\ 1/81.3\text{: lunar perturbation} \end{matrix}$$

$$x = \cos(L-\Delta\Omega) - 2\sin^2\frac{i'}{2}\sin L \sin \Delta\Omega$$

$$y = \left(1-2\sin^2\frac{i}{2}\right)\left[\sin(L-\Delta\Omega) - 2\sin^2\frac{i'}{2}\sin L\cos\Delta\Omega\right] + \sin i \sin i' \sin L$$

$$y' = \partial y/\partial i = \cos i \sin i' \sin L - 2\sin i \sin(L-\Delta\Omega) + 4\sin i \sin^2\frac{i'}{2}\sin L' \cos\Delta\Omega$$

$$U1 = \int_0^{2\pi} \sin u \cos u \, du/[1+e\cos(u-\omega)]^6$$

$$= 21\pi e^2 \sin 2\omega (1 + e^2/2)/[4(1-e^2)^{11/2}]$$

$$U2 = \int_0^{2\pi} \sin^2 u \, du/[1+e\cos(u-\omega)]^6$$

$$= [\pi/(1-e^2)^{11/2}][1 + (5-\tfrac{21}{4}\cos 2\omega)e^2 + \tfrac{3}{8}(5-7\cos 2\omega)e^4]$$

For GPS satellites, the orbits are nearly circular ($e \approx 0$), and Eq. (43) can be simplified to the following form:

$$\frac{\Delta P_3}{P} = \left(\frac{3}{2}\right)\left(\frac{n'}{n}\right)^2 \left(\frac{a'}{r'}\right)^3 \text{Rm cot i (yy')} \tag{44}$$

This algorithm has been incorporated into the computer program ELEMENT for an analysis of the orbit perturbations for the Phase III GPS satellites.

Figure 12 gives an example of orbit maintenance with this algorithm. This example is one of the 12 cases at 55-deg inclination of the Phase III system[16]. For this particular satellite, each correction requires 0.6 ft/sec or less in $\Delta V$, and the total $\Delta V$ used in the 10-yr period is about 7.5 ft/sec. The first and third corrections are caused by a slight overshoot at the upper bound (271 deg). This occasional overprediction seems to reveal a limitation of the first-order theory assumed in the new algorithm. To minimize the number of over- and under-predictions, a self-adjusting mechanism is incorporated. After an overshoot correction, as shown by $t_3$ in Fig. 12, the predicted maximum value of the variation in $\lambda_{ANX}$ in the next interval is scaled down by 10%. If the previous maximum $\delta\lambda_{ANX}$ is more than 10% undershoot, the next maximum $\delta\lambda_{ANX}$ is scaled up proportionally. This self-adjusting scheme is believed to be more efficient in computation than actual inclusion of those second-order terms of the perturbations which would significantly slow down the computation.

The long-term (10-yr) variations of the classical elements of the 12 GPS satellites and the orbit maintenance history may be found in Ref. 16. Results of those variations revealed the interesting fact that the value of inclination increases when the node $\Omega$ is between 0 and 180 deg, and the inclination decreases when the node is between 180 and 360 deg. The drift rate of inclination vanishes when the node is around 0 and 180 deg. With the analytical expansions derived in Part I, we are able to see that for this type of orbit ($e \approx 0$) the perturbations on inclination are mainly due to the sun and the moon. Neglecting terms of $e^2$ or higher, we obtain the averaged variational equation in inclination due to third-body perturbations from Eq. (7) as

$$\frac{di}{dt} = \frac{3}{4}\frac{n_3^2}{n}\left(\frac{a_3}{r_3}\right)^3 \left[\frac{1}{2}\cos i \sin 2i_3 \sin(\Omega - \Omega_3) + 2 \sin i \sin^2 i_3 \sin 2(\Omega - \Omega_3)\right] \tag{45}$$

Those parameters with a subscript 3 are of the third body. The node of the sun is zero and the node of the moon is confined to within $\pm 15$ deg on the earth equatorial plane where Eq. (45) is derived. With this equation, one can explain why the variation of inclination is a function of the right ascension of the ascending node $\Omega$.

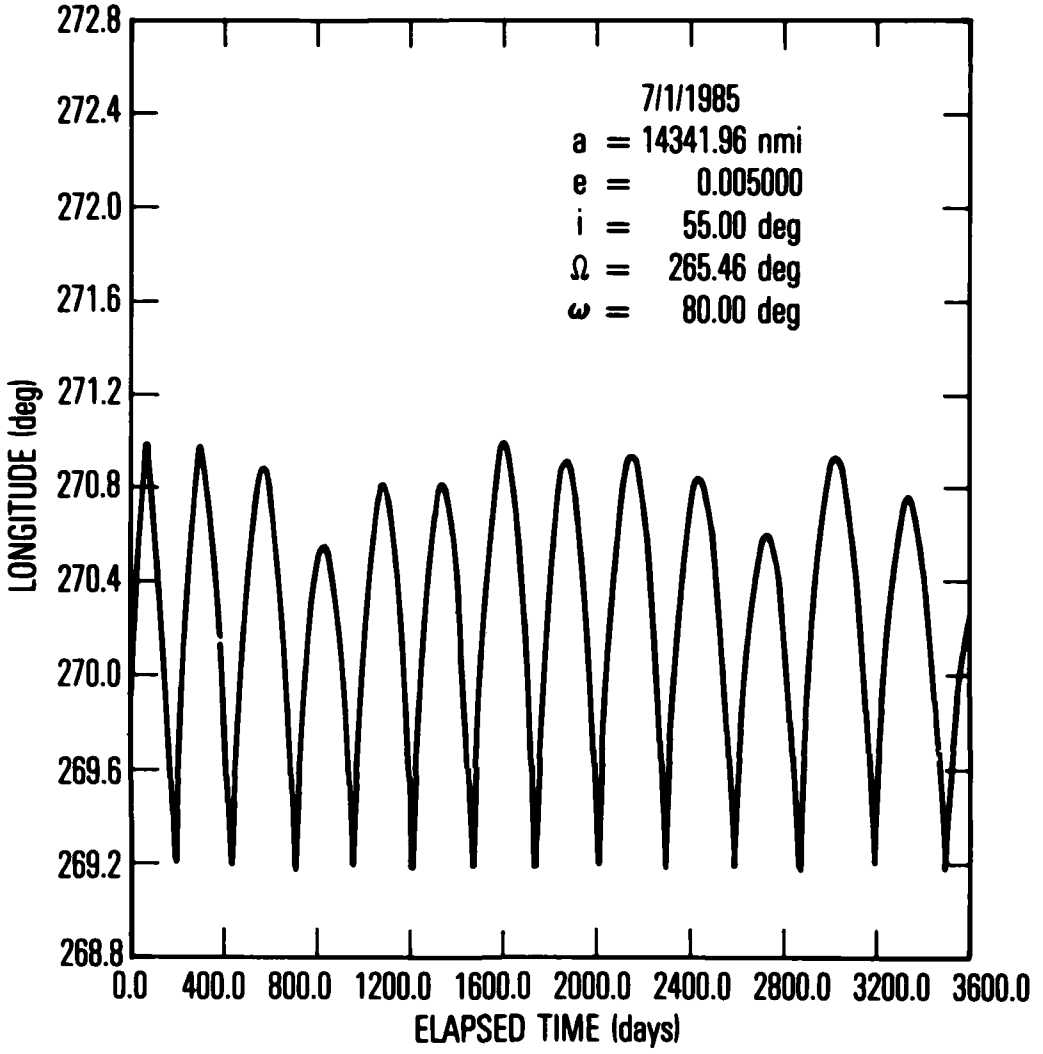


Fig. 12 Variations of $\lambda_{ANX}$ under Orbit Sustenance

The above example clearly indicates that the analytical solution has provided insight into the long-term variations of the orbit elements of the GPS satellites. This is particularly important for mission designers to understand the long-period characteristics of the orbit. Figure 13 shows how closely the first-order solution predicts the inclination variations of three GPS satellites in three different orbit planes. Even after 10 years, the error is only slightly over 10%. The computer time required to generate the 30 points of prediction is about 15 sec (CDC 7600).

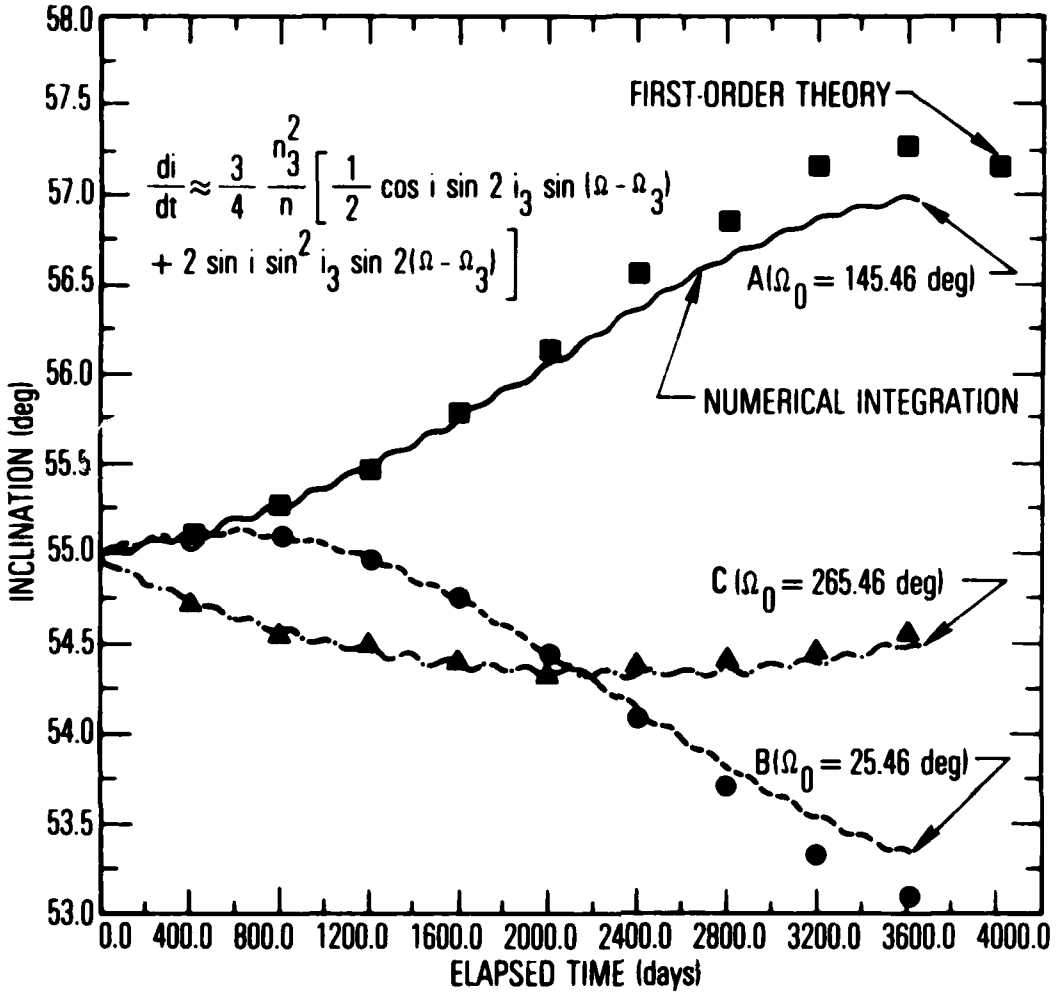


Fig. 13 Inclination Variation of the Phase III GPS Satellites

## CONCLUSIONS

The equations of variation perturbed by the sun-moon attractions are expanded by computer in terms of the familiar classical elements. The motions of the sun and the moon are represented by circular orbits with the nodal rate of the moon approximated by the projected mean value in the earth equatorial system. Results indicate that the first-order solution, analytically integrated with the secular part included in the reference orbit, can successfully handle the coupling between the sun-moon attraction and the oblateness effect. Good accuracy in predicting the variations of orbit elements up to 800 days has been demonstrated with examples of the GPS satellites. However, such accuracy of orbit prediction is limited to 100 days for high eccentricity orbits (e = 0.7). This is primarily because of the relatively large perturbations due to $J_2$ at high eccentricity which make the second-order terms important.

An algorithm applying the first-order solution has been developed to achieve the desired strategy of orbit maintenance for the GPS Phase III system. The result of a 10-yr simulation shows that the total $\Delta V$ required to maintain the longitude within $\pm 1$ deg is around 7.5 ft/sec with each correction of about 0.5 ft/sec. This algorithm will be useful in determining the time and magnitude of the orbit correction maneuvers for the GPS satellites. The analytical solution has helped to clarify the long-term variations of the GPS satellite orbits.

REFERENCES


1. Y. Kozai, "On the Effects of the Sun and the Moon upon the Motion of a Close Earth Satellite," Special Report No. 22, Smithsonian Institution Astrophysical Observatory, Cambridge, Mass., Mar. 1959.

2. W.M. Kaula, "A Development of the Lunar and Solar Disturbing Function," Astron. Journal, vol. 67, 1962, pp. 300.

3. P. Musen, A. Bailie, and E. Upton, "Development of the Lunar and Solar Perturbations in the Motion of an Artificial Satellite," NASA TN D-494, Jan. 1961.

4. J. Murphy and T. Felsentreger, "Analysis of Lunar and Solar Effects on the Motion of Close Earth Satellites," NASA TN D-3559, 1966.

5. R.H. Estes, "On the Analytic Lunar and Solar Perturbations of a Near Earth Satellite," NASA TM X-66000, Aug. 1972.

6. B. Kaufman, "Variation of Parameters and the Long-Term Behavior of Planetary Orbits," AIAA Paper No. 70-1055, presented at the AAS/AIAA Astrodynamics Conference at Santa Barbara, Ca., Aug. 1970.

7. C. Uphoff, "Numerical Averaging in Orbit Prediction," AIAA Paper No. 72-934, AIAA/AAS Astrodynamics Conference, Palo Alto, Ca., 11-12 Sept. 1972.

8. P. Cefola, A. Long, and G. Holloway, "The Long-Term Prediction of Artificial Satellite Orbits," AIAA Preprint 74-170, AIAA Twelfth Aerospace Science Meeting, Washington, D.C., Feb. 1974.

9. C.C. Chao, "A General Perturbation Method and Its Application to the Motions of the Four Massive Satellites of Jupiter," AIAA Paper No. 78-1385, presented at the AIAA/AAS Astrodynamics Conference at Palo Alto, Ca., Aug. 1978.

10. R.A. Broucke, Private Communication.

11. B.E. Baxter, "Notes on Program ELEMENT (Special Perturbations via An Averaged Disturbing Function)," The Aerospace Corporation, Rpt. No. TOR-0172(2441-02)-18, Sept. 1971.

12. B.E. Baxter, "$\Delta V$ Requirements for Ground Track Control of Q=2 Orbits," The Aerospace Corporation, Rpt. No. TOR-0074 (4901-03)-15, 7 June 1974.

13. S. Herrick, Astrodynamics, vol. 2, Van Nostrand Reinhold Co., London, 1972.

14. W.M. Kaula, Theory of Satellite Geodesy, Blaisdell Publishing Co., London, 1966.

15. A.J. Claus and A.G. Lubowe, "A High Accuracy Perturbation Method with Direct Application to Communication Satellite Orbit Prediction," Astronaut. Acta, vol. IX, Fasc. 5-6, 1963.

*16. C.C. Chao, "An Analysis of Long-Term Orbit Perturbations for the Phase III GPS Satellites," The Aerospace Corporation, Rpt. No. ATM-79(4476-01)-06, Feb. 1979.

## APPENDIX A

The package of series expansions used in this analysis is the latest version of the computerized series expansion package developed by R. Broucke of the University of Texas. After the terms are properly combined by hand, the two series may be rewritten as shown in Table A-2. This compact series may be useful for other types of analysis such as deriving the equations of variation from the averaged disturbing function [Eq. (2)] in the Delaunay variables. However, the results of Table A-1 will be used for continued series manipulation by computer to avoid any possible human error. We can then derive those partial derivatives of $(A^2 + B^2)$ and $(A^2 - B^2)$ with respect to the classical elements. Again, the operations were performed by the computer; results are shown in Tables A-3 through A-5. The nonzero series are denoted by the following symbols:

$$\text{IMW} = \frac{\partial(A^2 - B^2)}{\partial \omega} \quad , \quad \text{IPO} = \frac{\partial(A^2 + B^2)}{\partial \Omega} \quad , \quad \text{IMO} = \frac{\partial(A^2 - B^2)}{\partial \Omega}$$

$$\text{IPS} = \frac{\partial(A^2 + B^2)}{\partial \sin i} \quad , \quad \text{IPC} = \frac{\partial(A^2 + B^2)}{\partial \cos i} \quad ,$$

$$\text{IMS} = \frac{\partial(A^2 - B^2)}{\partial \sin i} \quad , \quad \text{IMC} = \frac{\partial(A^2 - B^2)}{\partial \cos i} \qquad \text{(A-1)}$$

*Aerospace internal correspondence. Not available for external distribution.

Table A-1

COMPUTER-GENERATED SERIES FOR $(A^2 + B^2)$ AND $(A^2 - B^2)$

```
     A2+B2=
+(+1-1/2*SI3**2-1/2*SI**2+3/4*SI**2*SI3**2)
+(+1*SI*CI*SI3*CI3)*COS(D)
+(+1/4*SI**2*SI3**2)*COS(2*D)
+(+1/4*SI**2+1/4*SI**2*CI3-1/8*SI**2*SI3**2)*COS(2*L-2*D)
+(-1/2*SI*CI*SI3-1/2*SI*CI*SI3*CI3)*COS(2*L-D)
+(+1/2*SI3**2-3/4*SI**2*SI3**2)*COS(2*L)
+(+1/2*SI*CI*SI3-1/2*SI*CI*SI3*CI3)*COS(2*L+D)
+(+1/4*SI**2-1/4*SI**2*CI3-1/8*SI**2*SI3**2)*COS(2*L+2*D)

     A2-B2=
+(+1/4*SI3**2-1/4*CI*SI3**2-1/8*SI**2*SI3**2)*COS(2*W-2*D)
+(+1/2*SI*SI3*CI3-1/2*SI*CI*SI3*CI3)*COS(2*W-D)
+(+1/2*SI**2-3/4*SI**2*SI3**2)*COS(2*W)
+(-1/2*SI*SI3*CI3-1/2*SI*CI*SI3*CI3)*COS(2*W+D)
+(+1/4*SI3**2+1/4*CI*SI3**2-1/8*SI**2*SI3**2)*COS(2*W+2*D)
+(+1/4+1/4*CI3-1/8*SI3**2+1/4*CI+1/4*CI*CI3-1/8*CI*SI3**2-1/8*SI**2-1/8*SI**2*CI
   3+1/16*SI**2*SI3**2)*COS(2*L-2*W-2*D)
+(+1/4*SI*SI3+1/4*SI*SI3*CI3+1/4*SI*CI*SI3+1/4*SI*CI*SI3*CI3)*COS(2*L-2*W-D)
+(+3/8*SI**2*SI3**2)*COS(2*L-2*W)
+(+1/4*SI*SI3-1/4*SI*SI3*CI3-1/4*SI*CI*SI3+1/4*SI*CI*SI3*CI3)*COS(2*L-2*W+D)
+(+1/4-1/4*CI3-1/8*SI3**2-1/4*CI+1/4*CI*CI3+1/8*CI*SI3**2-1/8*SI**2+1/8*SI**2*CI
   3+1/16*SI**2*SI3**2)*COS(2*L-2*W+2*D)
+(+1/4+1/4*CI3-1/8*SI3**2-1/4*CI-1/4*CI*CI3+1/8*CI*SI3**2-1/8*SI**2-1/8*SI**2*CI
   3+1/16*SI**2*SI3**2)*COS(2*L+2*W-2*D)
+(-1/4*SI*SI3-1/4*SI*SI3*CI3+1/4*SI*CI*SI3+1/4*SI*CI*SI3*CI3)*COS(2*L+2*W-D)
+(+3/8*SI**2*SI3**2)*COS(2*L+2*W)
+(-1/4*SI*SI3+1/4*SI*SI3*CI3-1/4*SI*CI*SI3+1/4*SI*CI*SI3*CI3)*COS(2*L+2*W+D)
+(+1/4-1/4*CI3-1/8*SI3**2+1/4*CI-1/4*CI*CI3-1/8*CI*SI3**2-1/8*SI**2+1/8*SI**2*CI
   3+1/16*SI**2*SI3**2)*COS(2*L+2*W+2*D)
```

$A2 + B2 = A^2 + B^2$

$A2 - B2 = A^2 - B^2$

Table A-2

SERIES OF $(A^2 + B^2)$ AND $(A^2 - B^2)$

$$A^2 + B^2 = \frac{1}{4}(1 + \cos^2 i)(1 + \cos^2 i_3) + \frac{1}{2}\sin^2 i \sin^2 i_3$$

$$+ \frac{1}{4}[\sin 2i \sin 2i_3 \cos \Delta\Omega + \sin^2 i \sin^2 i_3 \cos 2\Delta\Omega]$$

$$+ \frac{1}{2}\left(1 - \frac{3}{2}\sin^2 i\right)\sin^2 i_3 \cos 2u$$

$$+ \frac{1}{8}\sin^2 i\,[(1 + \cos i)^2 \cos 2(u - \Delta\Omega)$$

$$+ (1 - \cos i)^2 \cos 2(u + \Delta\Omega)]$$

$$+ \frac{1}{4}\sin 2i \sin i_3\,[(1 - \cos i_3)\cos(2u + \Delta\Omega)$$

$$- (1 + \cos i_3)\cos(2u - \Delta\Omega)]$$

$$A^2 - B^2 = \frac{1}{2}\sin^2 i\left(1 - \frac{3}{2}\sin^2 i_3\right)\cos 2\omega$$

$$+ \frac{1}{4}\sin 2i_3 \sin i\,[(1 - \cos i)\cos(2\omega - \Delta\Omega)$$

$$- (1 + \cos i)\cos(2\omega + \Delta\Omega)]$$

$$+ \frac{1}{8}\sin^2 i_3\,[(1 - \cos i)^2 \cos 2(\omega - \Delta\Omega)$$

$$+ (1 + \cos i)^2 \cos 2(\omega + \Delta\Omega)]$$

$$+ \frac{3}{8}\sin^2 i \sin^2 i_3\,[\cos 2(u - \omega) + \cos 2(u + \omega)]$$

$$+ \frac{1}{4}\sin^4 \frac{i_3}{2}\,[\sin^4 \frac{i}{2}\cos 2(u - \omega + \Delta\Omega) + \cos^4 \frac{i}{2}\cos 2(u + \omega + \Delta\Omega)]$$

$$+ \frac{1}{4}\cos^4 \frac{i_3}{2}\,[\sin^4 \frac{i}{2}\cos 2(u + \omega - \Delta\Omega) + \cos^4 \frac{i}{2}\cos 2(u - \omega - \Delta\Omega)]$$

$$+ \sin i \sin i_3 \sin^2 \frac{i_3}{2}\,[\sin^2 \frac{i}{3}\cos(2u - 2\omega + \Delta\Omega)$$

$$- \cos^2 \frac{i}{2}\cos(2u + 2\omega + \Delta\Omega)]$$

$$+ \sin i \sin i_3 \cos^2 \frac{i_3}{2}\,[\cos^2 \frac{i}{2}\cos(2u - 2\omega - \Delta\Omega)$$

$$- \sin^2 \frac{i}{2}\cos(2u + 2\omega - \Delta\Omega)]$$

Table A-3

SERIES OF IPO = $\partial(A^2 + B^2)/\partial\Omega$, IMO = $\partial(A^2 - B^2)/\partial\Omega$ AND IMS = $\partial(A^2 - B^2)/\partial \sin i$

```
     IPO=
+(-1*SI*CI*SI3*CI3)*SIN(D)
+(-1/2*SI**2*SI3**2)*SIN(2*D)
+(+1/2*SI**2+1/2*SI**2*CI3-1/4*SI**2*SI3**2)*SIN(2*L-2*D)
+(-1/2*SI*CI*SI3-1/2*SI*CI*SI3*CI3)*SIN(2*L-D)
+(-1/2*SI*CI*SI3+1/2*SI*CI*SI3*CI3)*SIN(2*L+D)
+(-1/2*SI**2+1/2*SI**2*CI3+1/4*SI**2*SI3**2)*SIN(2*L+2*D)

     IMO=
+(+1/2*SI3**2-1/2*CI*SI3**2-1/4*SI**2*SI3**2)*SIN(2*W-2*D)
+(+1/2*SI*SI3*CI3-1/2*SI*CI*SI3*CI3)*SIN(2*W-D)
+(+1/2*SI*SI3*CI3+1/2*SI*CI*SI3*CI3)*SIN(2*W+D)
+(-1/2*SI3**2-1/2*CI*SI3**2+1/4*SI**2*SI3**2)*SIN(2*W+2*D)
+(+1/2+1/2*CI3-1/4*SI3**2+1/2*CI+1/2*CI*CI3-1/4*CI*SI3**2-1/4*SI**2-1/4*SI**2*CI
   3+1/8*SI**2*SI3**2)*SIN(2*L-2*W-2*D)
+(+1/4*SI*SI3+1/4*SI*SI3*CI3+1/4*SI*CI*SI3+1/4*SI*CI*SI3*CI3)*SIN(2*L-2*W-D)
+(-1/4*SI*SI3+1/4*SI*SI3*CI3+1/4*SI*CI*SI3-1/4*SI*CI*SI3*CI3)*SIN(2*L-2*W+D)
+(-1/2+1/2*CI3+1/4*SI3**2+1/2*CI-1/2*CI*CI3-1/4*CI*SI3**2+1/4*SI**2-1/4*SI**2*CI
   3-1/8*SI**2*SI3**2)*SIN(2*L-2*W+2*D)
+(+1/2+1/2*CI3-1/4*SI3**2-1/2*CI-1/2*CI*CI3+1/4*CI*SI3**2-1/4*SI**2-1/4*SI**2*CI
   3+1/8*SI**2*SI3**2)*SIN(2*L+2*W-2*D)
+(-1/4*SI*SI3-1/4*SI*SI3*CI3+1/4*SI*CI*SI3+1/4*SI*CI*SI3*CI3)*SIN(2*L+2*W-D)
+(+1/4*SI*SI3-1/4*SI*SI3*CI3+1/4*SI*CI*SI3-1/4*SI*CI*SI3*CI3)*SIN(2*L+2*W+D)
+(-1/2+1/2*CI3+1/4*SI3**2-1/2*CI+1/2*CI*CI3+1/4*CI*SI3**2+1/4*SI**2-1/4*SI**2*CI
   3-1/8*SI**2*SI3**2)*SIN(2*L+2*W+2*D)

     IMS=
+(+1/2*SI3*CI3-1/2*CI*SI3*CI3)*COS(2*W-D)
+(-1*SI*SI3**2)*COS(2*W)
+(-1/2*SI3*CI3-1/2*CI*SI3*CI3)*COS(2*W+D)
+(+1/4*SI3+1/4*SI3*CI3+1/4*CI*SI3+1/4*CI*SI3*CI3)*COS(2*L-2*W-D)
+(+1/2*SI*SI3**2)*COS(2*L-2*W)
+(+1/4*SI3-1/4*SI3*CI3-1/4*CI*SI3+1/4*CI*SI3*CI3)*COS(2*L-2*W+D)
+(-1/4*SI3-1/4*SI3*CI3+1/4*CI*SI3+1/4*CI*SI3*CI3)*COS(2*L+2*W-D)
+(+1/2*SI*SI3**2)*COS(2*L+2*W)
+(-1/4*SI3+1/4*SI3*CI3-1/4*CI*SI3+1/4*CI*SI3*CI3)*COS(2*L+2*W+D)
```

## Table A-4

SERIES OF IPS - $\partial(A^2 + B^2)/\partial \sin i$, IPC - $\partial(A^2 + B^2)/\partial \cos i$ AND IMW - $\partial(A^2 - B^2)/\partial \omega$

```
     IPS=
+(+1*SI*SI3**2)
+(+1*CI*SI3*CI3)*COS(D)
+(-1/2*CI*SI3-1/2*CI*SI3*CI3)*COS(2*L-D)
+(-1*SI*SI3**2)*COS(2*L)
+(+1/2*CI*SI3-1/2*CI*SI3*CI3)*COS(2*L+D)

     IPC=
+(+1*CI-1/2*CI*SI3**2)
+(+1*SI*SI3*CI3)*COS(D)
+(-1/2*CI*SI3**2)*COS(2*D)
+(-1/2*CI-1/2*CI*CI3+1/4*CI*SI3**2)*COS(2*L-2*D)
+(-1/2*SI*SI3-1/2*SI*SI3*CI3)*COS(2*L-D)
+(+1/2*CI*SI3**2)*COS(2*L)
+(+1/2*SI*SI3-1/2*SI*SI3*CI3)*COS(2*L+D)
+(-1/2*CI+1/2*CI*CI3+1/4*CI*SI3**2)*COS(2*L+2*D)

     IMW=
+(-1/2*SI3**2+1/2*CI*SI3**2+1/4*SI**2*SI3**2)*SIN(2*W-2*D)
+(-1*SI*SI3*CI3+1*SI*CI*SI3*CI3)*SIN(2*W-D)
+(-1*SI**2+3/2*SI**2*SI3**2)*SIN(2*W)
+(+1*SI*SI3*CI3+1*SI*CI*SI3*CI3)*SIN(2*W+D)
+(-1/2*SI3**2-1/2*CI*SI3**2+1/4*SI**2*SI3**2)*SIN(2*W+2*D)
+(+1/2+1/2*CI3-1/4*SI3**2+1/2*CI+1/2*CI*CI3-1/4*CI*SI3**2-1/4*SI**2-1/4*SI**2*CI
   3+1/8*SI**2*SI3**2)*SIN(2*L-2*W-2*D)
+(+1/2*SI*SI3+1/2*SI*SI3*CI3+1/2*SI*CI*SI3+1/2*SI*CI*SI3*CI3)*SIN(2*L-2*W-D)
+(+3/4*SI**2*SI3**2)*SIN(2*L-2*W)
+(+1/2*SI*SI3-1/2*SI*SI3*CI3-1/2*SI*CI*SI3+1/2*SI*CI*SI3*CI3)*SIN(2*L-2*W+D)
+(+1/2-1/2*CI3-1/4*SI3**2-1/2*CI+1/2*CI*CI3+1/4*CI*SI3**2-1/4*SI**2+1/4*SI**2*CI
   3+1/8*SI**2*SI3**2)*SIN(2*L-2*W+2*D)
+(-1/2-1/2*CI3+1/4*SI3**2+1/2*CI+1/2*CI*CI3-1/4*CI*SI3**2+1/4*SI**2+1/4*SI**2*CI
   3-1/8*SI**2*SI3**2)*SIN(2*L+2*W-2*D)
+(+1/2*SI*SI3+1/2*SI*SI3*CI3-1/2*SI*CI*SI3-1/2*SI*CI*SI3*CI3)*SIN(2*L+2*W-D)
+(-3/4*SI**2*SI3**2)*SIN(2*L+2*W)
+(+1/2*SI*SI3-1/2*SI*SI3*CI3+1/2*SI*CI*SI3-1/2*SI*CI*SI3*CI3)*SIN(2*L+2*W+D)
+(-1/2+1/2*CI3+1/4*SI3**2-1/2*CI+1/2*CI*CI3+1/4*CI*SI3**2+1/4*SI**2-1/4*SI**2*CI
   3-1/8*SI**2*SI3**2)*SIN(2*L+2*W+2*D)
```

Table A-5

SERIES OF IMC = $\partial(A^2 - B^2)/\partial \cos i$

```
      IMC=
     +(-1/4*SI3**2+1/4*CI*SI3**2)*COS(2*W-2*D)
     +(-1/2*SI*SI3*CI3)*COS(2*W-D)
     +(-1*CI+1/2*CI*SI3**2)*COS(2*W)
     +(-1/2*SI*SI3*CI3)*COS(2*W+D)
     +(+1/4*SI3**2+1/4*CI*SI3**2)*COS(2*W+2*D)
     +(+1/4+1/4*CI3-1/8*SI3**2+1/4*CI+1/4*CI*CI3-1/8*CI*SI3**2)*COS(2*L-2*W-2*D)
     +(+1/4*SI*SI3+1/4*SI*SI3*CI3)*COS(2*L-2*W-D)
     +(-1/4*CI*SI3**2)*COS(2*L-2*W)
     +(-1/4*SI*SI3+1/4*SI*SI3*CI3)*COS(2*L-2*W+D)
     +(-1/4+1/4*CI3+1/8*SI3**2+1/4*CI-1/4*CI*CI3-1/8*CI*SI3**2)*COS(2*L-2*W+2*D)
     +(-1/4-1/4*CI3+1/8*SI3**2+1/4*CI+1/4*CI*CI3-1/8*CI*SI3**2)*COS(2*L+2*W-2*D)
     +(+1/4*SI*SI3+1/4*SI*SI3*CI3)*COS(2*L+2*W-D)
     +(-1/4*CI*SI3**2)*COS(2*L+2*W)
     +(-1/4*SI*SI3+1/4*SI*SI3*CI3)*COS(2*L+2*W+D)
     +(+1/4-1/4*CI3-1/8*SI3**2+1/4*CI-1/4*CI*CI3-1/8*CI*SI3**2)*COS(2*L+2*W+2*D)
```

Note that the designed package cannot take partial differentiation directly with respect to the inclination i, which is treated as a polynomial variable. Thus, the intermediate parameters sin i and cos i are used with the following relations to complete the differentiation.

$$\frac{\partial F}{\partial i} = \frac{\partial F}{\partial \sin i} \cos i - \frac{\partial F}{\partial \cos i} \sin i \qquad \text{(A-2)}$$

Note also that the printed series are in FORTRAN language; they can be punched out and directly inserted into FORTRAN programs.

## APPENDIX B

### $J_2$ Perturbation

$$\frac{de}{dt} = -\frac{45}{32} n \epsilon_2^2 e(1-e^2) \sin^2 i \sin 2\omega \left(\frac{14}{15} - \sin^2 i\right)$$

$$\frac{di}{dt} = \frac{45}{64} \epsilon_2^2 n e^2 \sin 2i \left(\frac{14}{15} - \sin^2 i\right) \sin 2\omega$$

$$\frac{d\Omega}{dt} = -\frac{3}{2} n \epsilon_2 \cos i - \frac{9}{4} n \epsilon_2^2 \cos i \left[\frac{3}{2} - \frac{5}{6} \sin^2 i + \left(\frac{1}{6} + \frac{5}{24} \sin^2 i\right) e^2 + \left(\frac{7}{12} - \frac{5}{4} \sin^2 i\right) e^2 \cos 2\omega\right] \qquad \text{(B-1) (cont.)}$$

$$\frac{d\omega}{dt} = \frac{3}{2} n \epsilon_2 \left(2 - \frac{5}{2} \sin^2 i\right) - \frac{9}{4} n \epsilon_2^2 \left| 2 - \frac{23}{4} \sin^2 i + \frac{55}{16} \sin^4 i \right.$$

$$+ \frac{e^2}{4} \left(7 - \frac{9}{2} \sin^2 i + \frac{75}{4} \sin^4 i\right) + \frac{\cos 2\omega}{4} \left[\left(7 - \frac{15}{2} \sin^2 i\right) \sin^2 i \right.$$

$$\left. \left. + e^2 \left(7 + 5 \sin^2 i - \frac{45}{4} \sin^4 i\right)\right]\right| \qquad \text{(B-1)}$$

where

$$\epsilon_2 = J_2 \left(R_e^2/p^2\right)$$

$$p = a(1-e^2)$$

$R_e$ = equatorial radius of earth

$J_3$ Perturbation

$$\frac{de}{dt} = n\epsilon_3 (1-e^2) \cos\omega \sin i (1-5 \cos^2 i)$$

$$\frac{di}{dt} = n\epsilon_3 e \cos\omega \cos i (5 \cos^2 i - 1)$$

$$\frac{d\Omega}{dt} = n\epsilon_3 e \sin\omega \cot i (15 \cos^2 i - 11)$$

$$\frac{d\omega}{dt} = n\epsilon_3 \frac{(1 + 4e^2)}{e} \sin\omega \sin i (5 \cos^2 i - 1) - \frac{d\Omega}{dt} \cos i \qquad \text{(B-2)}$$

where

$$\epsilon_3 = 3/8 \, (R_e/p)^3 \, J_3$$

$J_4$ Perturbation

$$\frac{de}{dt} = -n\epsilon_4 e(1-e^2) \sin 2\omega \sin^2 i(7 \cos^2 i - 1)$$

$$\frac{di}{dt} = \frac{1}{2} n\epsilon_4 e^2 \sin 2\omega \sin 2 i (7 \cos^2 i - 1)$$

$$\frac{d\Omega}{dt} = n\epsilon_4 \cos i \left| 2 (7 \cos^2 i - 3) + e^2 [7 \cos^2 i - 1 \right.$$

$$\left. + 4 \sin^2\omega (7 \cos^2 i - 4)] \right| \qquad \text{(B-3)}$$

(cont.)

$$\frac{d\omega}{dt} = -2n\epsilon_4 \left\{ 8 - 28 \sin^2 i + 21 \sin^4 i - \sin^2\omega \sin^2 i \,(7\cos^2 i - 1) + e^2 \left[ 6 - 14 \sin^2 i + \frac{63}{8}\sin^4 i + \sin^6\omega \left(6 - 35 \sin^2 i + \frac{63}{2}\sin^4 i\right)\right]\right\} \tag{B-3}$$

where

$$\epsilon_4 = 15/32 \,(R_e/p)^4 \, J_4$$

APPENDIX C

Table C-1

THE $F_{\ell mp}$ AND $G_{\ell pq}$ FUNCTIONS

$$F_{221} = \frac{3}{2}\sin^2 i, \quad F_{220} = \frac{3}{4}(1+\cos i)^2$$

$$F_{321} = \frac{15}{8}\sin i\,(1-2\cos i - 3\cos^2 i)$$

$$F_{322} = -\frac{15}{8}\sin i\,(1+2\cos i - 3\cos^2 i)$$

$$F_{311} = \frac{15}{16}\sin^2 i\,(1+3\cos i) - \frac{3}{4}(1+\cos i)$$

$$F_{330} = \frac{15}{8}(1+\cos i)^3$$

$$F_{421} = \frac{105}{8}\sin^2 i \cos i\,(1+\cos i) - \frac{15}{8}(1+\cos i)^2$$

$$F_{440} = \frac{105}{16}(1+\cos i)^4$$

$$G_{211} = 1.5e + 1.6875e^3 + 2.0390625e^5 + 2.3289388e^7 + 2.587323e^9 + 2.822341e^{11} + 3.03933758e^{13} + 3.2418959e^{15} + 3.43255448e^{17} + 3.6131875e^{19} \ldots\ldots$$

$$G_{20-1} = -0.5e + 0.0625e^3 - 0.0130208e^5 - 0.77582465 \times 10^{-2} e^7 - 6.16930 \times 10^{-3} e^9 - 4.96735185 \times 10^{-3} e^{11} - 4.0929341 \times 10^{-3} e^{13} - 3.44089913 \times 10^{-3} e^{15} + \ldots\ldots$$

Table C-1

THE $F_{\ell mp}$ AND $G_{\ell pq}$ FUNCTIONS (Continued)

$$G_{310} = 1 + 2e^2 + 3.734375e^4 + 5.769097222e^6 + 8.096605089e^8 + 10.6829796e^{10} + 13.50467544e^{12} + 16.54355294e^{14} + 19.7851081e^{16} + 23.21740226e^{18} + 26.83038574e^{20} + \ldots\ldots$$

$$G_{322} = 1.375e^2 + 3.0625e^4 + 5.099283854e^6 + 7.427332899e^8 + 10.01418813e^{10} + 12.83625022e^{12} + 15.87540617e^{14} + 19.11717618e^{16} + 22.54963923e^{18} + 26.16275785e^{20} + \ldots\ldots$$

$$G_{30-2} = 0.125e^2 + 0.0208333e^4 + 0.0179036e^6 + 0.0127713e^8 + 0.009776e^{10} + 0.0077966e^{12} + 0.0064085e^{14} + \ldots\ldots$$

$$G_{41-1} = 0.5e + 2.0625e^3 + 4.794271e^5 + 7.048177e^7 + 7.416341e^9 + 6.046672e^{11} + 3.999685e^{13} + 2.208745e^{15} + 1.037865e^{17} + 0.420094e^{19} + \ldots\ldots$$

$$G_{410} = 1 + e^2 + 4.0625e^4 + 6.3125e^6 + 6.566406e^8 + 5.257813e^{10} + 3.438477e^{12} + 1.913086e^{14} + 0.923584e^{16} + 0.389633e^{18} + 0.143613e^{20} + \ldots\ldots$$

$$G_{421} = 2.5e + 8.4375e^3 + 18.65885e^5 + 26.132813e^7 + 26.069336e^9 + 20.032104e^{11} + 12.389781e^{13} + 6.332082e^{15} + 2.716932e^{17} + 0.986036e^{19} + \ldots\ldots$$

$$G_{40-2} = 0.5e^2 - 0.3333333e^4 - 0.125e^6 + 0.338542e^8 + 0.314453e^{10} + 0.093099e^{12} - 0.048706e^{14} - 0.062805e^{16} - 0.027145e^{18} - \ldots\ldots$$

Table C-2

VALUES OF LOW-ORDER (FOURTH) HARMONICS OF EARTH GRAVITATION POTENTIAL (WGS 72 MODEL)

Zonal Harmonics

$J_2 = 1082.61579\ E\text{-}6^*$

$J_3 = -2.53881\ E\text{-}6$

$J_4 = -1.65597\ E\text{-}6$

Tesseral Harmonics

| | |
|---|---|
| $C_{22} = 1.5765\ E\text{-}6$ | $S_{22} = -9.0602\ E\text{-}7$ |
| $C_{31} = 2.2181\ E\text{-}6$ | $S_{31} = 2.8843\ E\text{-}7$ |
| $C_{32} = 3.1196\ E\text{-}7$ | $S_{32} = 02.2055\ E\text{-}7$ |
| $C_{33} = 9.8324\ E\text{-}8$ | $S_{33} = 1.9611\ E\text{-}7$ |
| $C_{42} = 7.6894\ E\text{-}8$ | $S_{42} = 1.4562\ E\text{-}7$ |
| $C_{44} = -4.0641\ E\text{-}9$ | $S_{44} = 6.7006\ E\text{-}9$ |

*E-6 = $x10^{-6}$